The Mass Budget of Arctic Glaciers

Extended abstracts

Workshop, 13-15 January 2005, Pontresina (Switzerland)

IASC Working group on Arctic Glaciology

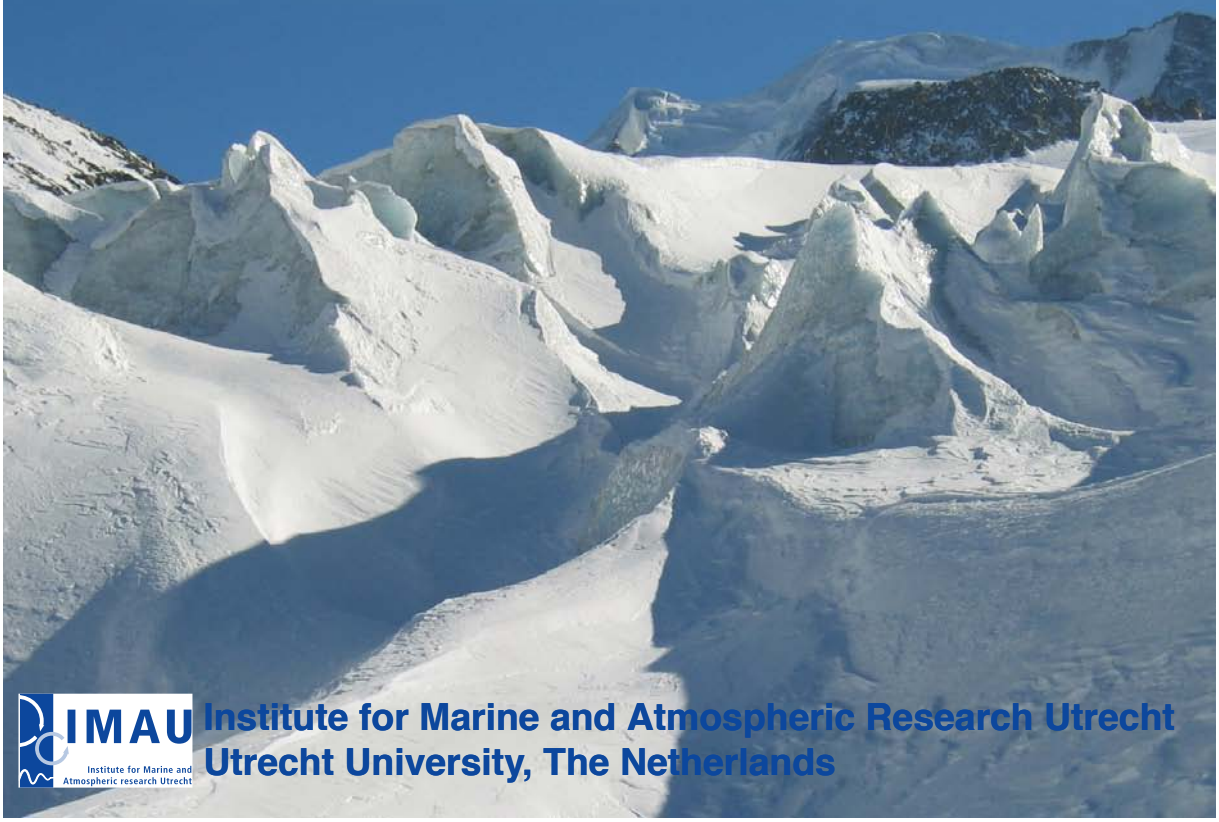

IMAU Institute for Marine and Atmospheric research Utrecht

Institute for Marine and Atmospheric Research Utrecht
Utrecht University, The Netherlands

The mass budget of Arctic Glaciers

Extended abstracts

Workshop, 13-15 January 2005, Pontresina (Switzerland)

IASC Working group on Arctic Glaciology

Organised by J. Oerlemans

Institute for Marine and Atmospheric Research Utrecht
Utrecht University, The Netherlands

CONTENTS

Preface 5
Johannes Oerlemans

Program 7

List of participants 9

Mass balance observations on the Aldegonda Glacier in 2003/2004 placement 11
B.R. Mavlyudov and I.Y. Solovyanova

Meteorological measurements and the surface energy balance on McCall Glacier, Alaska 14
Lisette Klok and Matt Nolan

Deriving glacier mass balance from ELA and AAR on Storglaciären 18
Dirk-Sytze Kootstra, Regine Hock and Peter Jansson

Simple modelling of calving glaciers 20
Johannes Oerlemans

On elevation changes of Svalbard glaciers 25
J.O. hagen, T. Eiken and K. Melvold

Automatic Weather Stations in the ablation zone of the west Greenland ice sheet 28
Michiel van den Broeke, Paul Smeets, Wim Boot, Johannes Oerlemans, Wouter Greuell and Roderik van de Wal

Glacier Velocities in the Canadian High Arctic from RADARSAT-1 Speckle Tracking 33
N.H. Short and A.L. Gray

Use of time-lapse cameras on automatic weather stations 38
Matt Nolan

Reconstruction of past accumulation rates in an alpine firn region: Fiescherhorn, Swiss Alps 40
Aurel Schwerzmann, Martin Funk, Heinz Blatter, Martin Lüthi, Margit Schwikowski, Anne Palmer

Elevation change of the West Greenland ice-sheet margin near Kangerlussuaq 2000-2003 43
Andreas P. Ahlstrøm, Niels Reeh, Lars Stenseng and Rene Forsberg

Comparative simulations of snow and superimposed ice at the Kongsvegen glacier, Svalbard 50
Stefan Erath, Friedrich Obleitner, Jack Kohler, Wouter Greuell and Kjetil Melvold

PREFACE

It has become a tradition that the Working Group on Arctic Glaciology of the International Arctic Science Committee (IASC-WAG) organizes an annual workshop on the mass budget of Arctic glaciers. However, in 2004 this workshop was embedded in a much larger event, namely the conference on Arctic Glaciology, organized together with the International Glaciological Society in Geilo, Norway (August 2004).
In January 2005 the tradition was picked up again, and a number of glaciologists gathered in Pontresina, Switzerland for a three-day workshop (13-15 January). Two days were dedicated to the presentation of ongoing research work and discussion, and one day to an excursion to the Automatic Weather Station on the Morteratschgletscher.
A number of extended abstracts from the presentations has been collected in this little book, together with the programme and the list of participants. The contributions were not reviewed, but hopefully provide some useful information and inspiration for further studies and collaboration.

I like to thank the Institute for Marine and Atmospheric Research of Utrecht University (IMAU) for the generous support that made it possible to organize the workshop and print this report. I am also grateful to Carleen Tijm-Reijmer for her help with the editorial work.

Johannes Oerlemans
Chairman, IASC Working Group on Arctic Glaciology

PROGRAM

Thursday 13 January

- 13:00 - 13:15 Welcome and practical announcements. *J. Oerlemans chairman IASC-WAG.*
- 13:15 - 13:45 Deriving glacier mass balance from ELA and AAR on Storglaciären. *D.-S. Kootstra, R. Hock, P. Jansson.*
- 13:45 - 14:15 Mass balance observations on the Aldegonda Glacier (Svalbard) in 2003/2004. *B.R. Mavlyudov & I.Y. Solovjanova.*
- 14:15 - 14:45 New data of geometry changes on Svalbard glaciers. *J.O. Hagen.*

14:45 - 15:15 Coffee break

- 15:15 - 15:45 The surface albedo of Kongsvegen as derived from MODIS satellite data. *W. Greuell.*
- 15:45 - 16:15 Glacier velocities in the Canadian High Arctic from RADARSAT-1 data. *N.H. Short & A.L. Gray.*
- 16:15 - 16:45 Mass balance measurements and records in Alaska. *M. Nolan.*
- 16:45 - 17:00 Availability of data from Storglaciären. *P. Holmlund.*
- 17:00 - 17:15 Introduction to the excursion on saturday (AWS on the Morteratschgletscher). *J. Oerlemans.*

Friday 14 January

- 09:00 - 09:30 Comparative simulations of the mass and energy budget at the equilibrium line of Kongsvegen glacier, Svalbard. *S. Erath & F. Obleitner.*
- 09:30 - 10:00 Modelling superimposed ice formation at a high Arctic glacier, Svalbard: an intercomparison of approaches. *J.L. Wadham.*
- 10:00 - 10:30 Elevation change of the West Greenland ice-sheet margin near Kangerlussuaq 2000-2003. *A. Ahlstrøm.*

10:30 - 11:00 Coffee break

- 11:00 - 11:30 Automatic Weather Stations in the ablation zone of the Greenland Ice Sheet. *M.R. van den Broeke et al.*
- 11:30 - 12:00 Meteorological measurements and the surface energy balance on McCall Glacier, Alaska. *E.J. Klok and M. Nolan.*
- 12:00 - 12:30 Recent glaciological studies on Hans Glacier, Southern Svalbard: preliminary results and perspectives. *J. Jania.*

12:30 - 13:45 Lunch

- 13:45 - 14:15 Studies of the Crystal Cave within Hansbreen, Svalbard, using speleological technique during winter 2003/2004 (MOVIE). *S. Kostka, T. Lekarski, P. Glowacki, J. Jania.*

- 14:15 - 14:45 Reconstruction of past accumulation rates in high alpine firn regions. *H. Blatter.*
- 14:45 - 15:15 Ice-coring in caves. *P. Holmlund.*

15:15 - 15:45 Coffee break

- 15:45 - 16:15 Form and flow of large ice caps in the Russian and Canadian high Arctic islands. *J.A. Dowdeswell.*
- 16:15 - 16:45 Simple modeling of calving glaciers. *J. Oerlemans.*
- 17:00 - 18:30 Plenary discussion on a new IASC-WAG programme for the IPY (and beyond). *GLACIODYN.*
- 20:30 - 22:00 **National representatives meeting**

Saterday 15 January

Excursion to the Morteratschgletscher

LIST OF PARTICIPANTS

1. A. Ahlstrøm (aa@oersted.dtu.dk)
   Technical University of Denmark, Copenhagen
2. H. Blatter (heinz.blatter@env.ethz.ch)
   ETH-Zürich, Switzerland
3. M.R. van den Broeke (m.r.vandenbroeke@phys.uu.nl)
   IMAU, Utrecht University, Netherlands
4. J.A. Dowdeswell (jd16@cam.ac.uk)
   Scott Polar Research Institute, Cambridge, U.K.
5. S. Erath
   Universität Innsbruck, Austria
6. U. Fischer (ufischer@vaw.baug.ethz.ch)
   VAW ETH-Zürich, Switzerland
7. W. Greuell (w.greuell@phys.uu.nl)
   IMAU, Utrecht University, Netherlands
8. R. Hock (regine.hock@natgeo.su.se)
   University of Stockholm, Sweden
9. J.O. Hagen (j.o.m.hagen@geo.uio.no)
   University of Oslo, Norway
10. P. Holmlund (pelle@natgeo.su.se)
    University of Stockholm, Sweden
11. J. Jania (jjania@us.edu.pl)
    University of Silesia, Sosnowiec, Poland
12. E.J. Klok (klok@knmi.nl)
    IMAU, Utrecht University, Netherlands
13. M. Kuhn (michael.kuhn@uibk.ac.at)
    Universität Innsbruck, Austria
14. A. Mittermeier
    University of Alaska, Fairbanks, Alaska
15. M. Nolan (fnman@uaf.edu)
    University of Alaska, Fairbanks, Alaska
16. F. Obleitner (friedrich.obleitner@uibk.ac.at)
    Universität Innsbruck, Austria
17. A. Ohmura (atsumu.ohmura@env.ethz.ch)
    ETH-Zürich, Switzerland
18. J. Oerlemans (j.oerlemans@phys.uu.nl)
    IMAU, Utrecht University, Netherlands
19. F. Paul (fpaul@geo.unizh.ch)
    Universität Zürich, Switzerland
20. T. Schuler (thomas.schuler@geo.uio.no)
    University of Oslo, Norway
21. N. Short (naomi.short@ccrs.nrcan.gc.ca)
    Canada Centre for Remote Sensing, Ottawa
22. I. Solovjanova (solir22@mail.ru)
    Arctic and Antarctic Res. Inst., St-Petersburg, Russia
23. J.L. Wadham (j.l.wadham@bristol.ac.uk)
    University of Bristol, U.K.

ABSTRACTS

MASS BALANCE OBSERVATIONS ON THE ALDEGONDA GLACIER IN 2003/2004 PLACEMENT

B. R. MAVLYUDOV[1] AND I. Y. SOLOVYANOVA[2]

[1]Institute of Geography Russian Academe of Science. Staromonetny, 29. Moscow, Russia
[2]Arctic and Antarctic Research Institute. Bering, 38. St-Petersburg. Russia

Mass balance of the glaciers of Spitsbergen is an important and reliably indicator of climate change in subarctic areas. In 2003 mass balance and water balance measurements were initiated in the basin of Aldegonda Glacier (a poly-thermal valley glacier in West Spitsbergen), about 10 km from the Russian settlement Barentsburg the program of mass balance and water balance measurements of glacial basin has begun. Snow surveys were carried out in May 2003 and 2004.
Aldegonda Glacier is located on the western coast of Grønfjord (Nordenskjold Land). It flows in a west-east direction and has a length of about 3 km, and a width up to 2 km (Fig. 1). The maximum ice thickness is 216 m (according to radio-echo sounding). In the 20th century the glacier has retreated from the coast over a distance of 2 km. The low point of the glacier tongue is located at 80 m asl, and the highest points are about 600 m asl; the average surface elevation of the glacier is about 275 m asl.

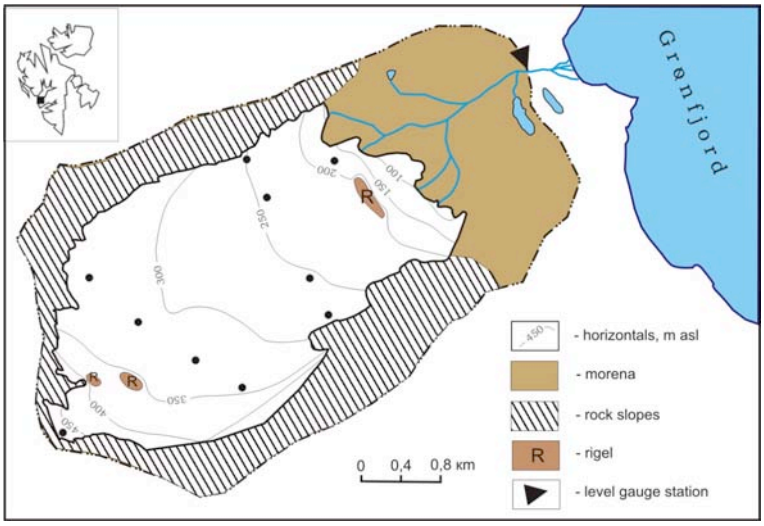

Figure 1. Aldegonda Glacier basin and location on Spitsbergen

Meteorological conditions for 2003 - 2004 and some characteristics of Aldegonda Glacier are summarized in the Table 1.
The winter balance (B_w) of Aldegonda glacier was determined from snow surveys. The snow cover distribution on the glacier area was uniform in both years. In 2003 the mean snow thickness was 125 cm (85 - 218 cm); the maximum snow thickness

was observed in the slope parts of the glacier. The mean snow density was 0.39 g/cm^3 (0.34 - 0.55 g/ cm^3, C_v = 0.20). In 2004 the mean snow thickness was 124 cm (38 - 176 cm), the mean density of snow was 0.36 g/cm^3 (0.33-0.39 g/cm^3). The mean water storage in the snow pack in the spring of 2003 was 56.7 cm w.e., in the spring of 2004 it was 48.6 cm w.e. In 2003 and 2004 there was no significant correlation between snow thickness and elevation (in the spring of 1978 the correlation of snow depth with height was r = 0,96).

Table 1. The data from Barentsburg meteorological stations and some characteristics of Aldegonda Glacier.

	2002/2003	**2003/2004**
Air temperature, °C		
June	2,5	2,6
July	6,2	5,2
August	5,9	4,8
Mean summer temperature	4,9	4,2
Precipitation sum, mm		
summer	67,4	63,4
winther	537	331
Ablation period, days	90	80
Bw (cm w.e.)	56,0	48,5
Bs (cm w.e.)	-226,8	-207,8
Bn (cm w.e.)	-170,8	-159,3
Net balance (106 m3)	12,94	11,99
ELA (m)	700	700

The net balance (B_n) of Aldegonda Glacier in 2002/03 was -170.8 cm w.e. (Table 1); in 2003/04 it was 159.3 cm w.e. In 2002/2003 it ranged from -366 cm w.e. at the glacier tongue to -69 cm w.e. at an elevation of 450 m asl. In 2003/2004 the specific balance ranged from -348 cm w.e. to -109 cm w.e. These number show make clear that the glacier lost a large amount of mass (Fig. 2).

The summer balance (B_s) was calculated by subtracting the winter balance ($+B_w$) from the net balance ($\pm B_n$). In 2002/03 the summer balance was equal to -227 cm w.e.; in 2003/2004 it was - 208 cm w.e.

Accumulation on Aldegonda Glacier correlates well with the sum of winter precipitation. According to the Barentsburg meteorological station the sum of precipitation in the cold period of 2002/2003 was 579 mm, and the specific accumulation on the glacier as obtained from snow surveys was equal to 561 mm. Based on the assumption that this good agreement holds in general, the net balance of the glacier was calculated for the entire period for which data from the meteorological station were available (1912-2002). The summer ablation was calculated with Mihalev's empirical formula for Spitsbergen:

$$A = (T_{VI\text{-}VIII} + 8.7)^3,$$

where A is ablation in mm w.e. and $T_{VI\text{-}VIII}$ is the mean summer air temperature in °C.

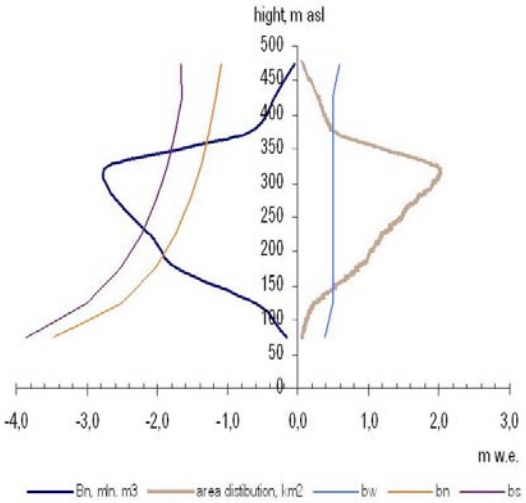

Figure 2. Mean values of specific winter, summer and net balance as a function of altitude on Aldegonda Glacier.

The average net balance for period from 1911 to 2003 was equal to -82 cm w.e., and for period from 1936 to 2003 equal to -77 cm w.e. (Fig. 3). A topographical map from 1936 and our GPS survey of the glacier surface in 2002 has allowed us to estimate the glacier surface change for the period of 67 years: the glacier surface has lowered by 64 m on average. The mean net balance of the glacier was equal to -86 cm w.e., which is rather close to the reconstructed value mentioned above (-77 cm w.e.).

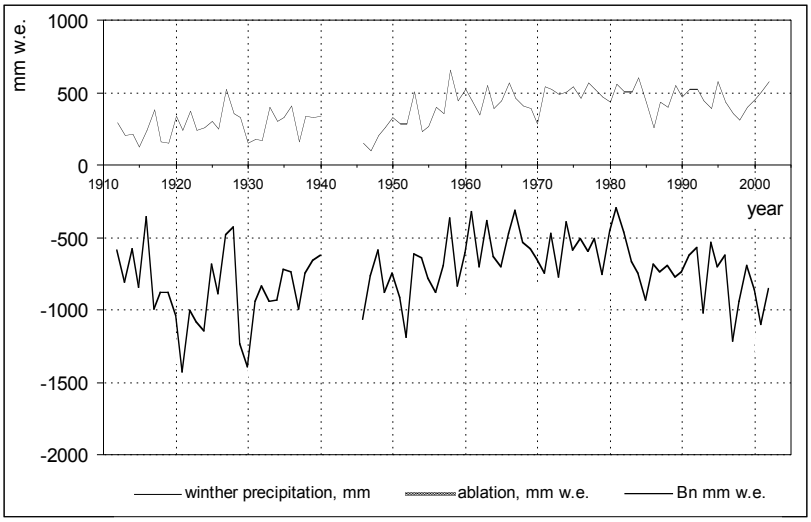

Figure 3. Winter precipitation and reconstructed ablation and net balance.

METEOROLOGICAL MEASUREMENTS AND THE SURFACE ENERGY BALANCE ON MCCALL GLACIER, ALASKA

LISETTE KLOK* AND MATT NOLAN

Water and Environmental Research Institute, Institute of Northern Engineering, University of Alaska Fairbanks, USA.
*Visiting scientist at IMAU, Utrecht University, the Netherlands

Introduction

We examined meteorological data of a summer period (27 May to 20 August 2004) of two automatic weather stations (AWS) to gain more knowledge about the relationship between climate and ice melt on McCall Glacier in Alaska. This research is part of the US National Science Foundation's Freshwater Initiative, which aims to document changes in the freshwater inputs in the Arctic hydrological system and how they relate to climate change. Average weather conditions, the energy balance and total ablation for the summer period are briefly described in this abstract.

Figure 1. Two automatic weather stations: JJMC on the glacier tongue of McCall Glacier (left) and AHAB on a mountain ridge above the glacier (right). (Photos taken in May 2004 by Matt Nolan.)

McCall Glacier is located at 69˚18'N 143˚48' W, in the Romanzof Mountains of the eastern Brooks Range in northeast Alaska. Since 1890, it has retreated about 800 m, and currently, its length is 7.5 km, and its area 6.5 km^2. The glacier elevation ranges from about 1400 to 2400 m a.s.l.
One AWS (JJMC) is located in the ablation area on the glacier tongue at 1715 m a.s.l. and another (AHAB) at 2415 m a.s.l. on a mountain ridge several hundred meters above the McCall Glacier (Fig. 1). These AWS were installed in 2003 by the Water and Environmental Research Institute, University of Alaska, Fairbanks.

JJMC is a floating station such that the heights of the instruments remain constant throughout the ablation season. Near JJMC, two ablation stakes measure surface melt and a sonic height ranger (Campbell SR50) measures ablation and snowfall. For our analysis, we used 15-minute averages of air temperature (2.06 m, fine wire couple), relative humidity (2.06 m, HMP45AC Vaisala with a Young radiation shield), wind speed and direction (3.05 m, Met One 034B) and the four radiation components (1.44 m, Kipp & Zonen) from this station. Besides, we used data from a thermistor-string that measures ice temperatures every 0.5 m until a depth of 13.5 m. From AHAB, we used hourly averages of air temperature and humidity (3.0 m, HMP45AC Vaisala with a Young radiation shield), wind speed (3.0m, Met One 034B), and air pressure (Vaisala CS105).

Analysis of meteorological measurements

Between 27 May and 20 August 2004, daily mean temperature at AHAB and JJMC ranged between –8 and +12 ˚C. The average air temperature at JJMC was 5.3 ˚C and at AHAB 4.2 ˚C. The temperature gradient between JJMC and AHAB is thus very small (–0.2 K per 100 m altitude). 2004 was exceptional warm summer in Alaska. For Barrow (northern Alaska), it was the second warmest summer on record. The average wind speed at AHAB was 3.6 m s^{-1} and at JJMC 3.1 m s^{-1}. The mean relative humidity was 69% and 72%, respectively.

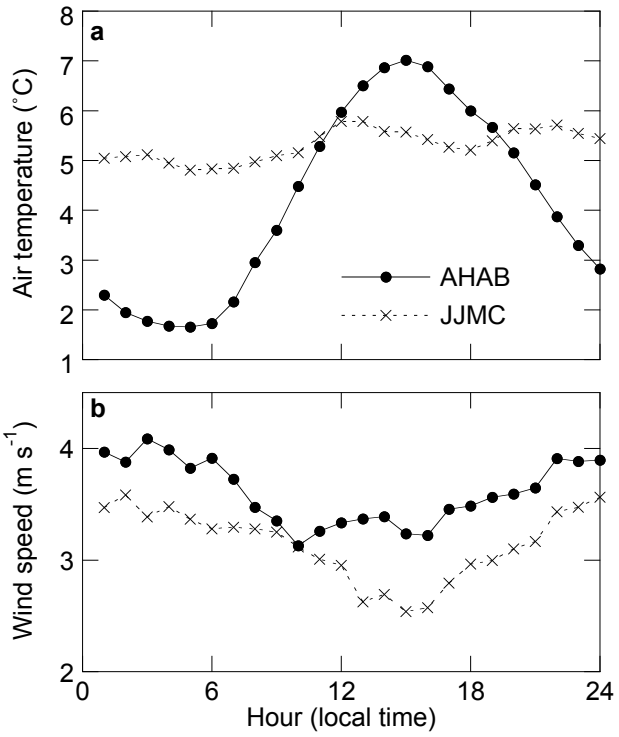

Figure 2. Mean daily cycle in air temperature (A) and wind speed (B) at AHAB and JJMC over the period 27 May to 20 August, 2004.

Fig. 2 shows mean daily variation in air temperature and wind speed for JJMC and AHAB. The air temperature at AHAB shows a clear daily cycle with a daily range of 5.3 ˚C. Contrarily, JJMC hardly shows a daily variation in temperature. This can be explained by the cooling effect of the glacier. The temperature at JJMC is influenced by an almost constant surface temperature at melting point. Another interesting result is the absence of a wind speed maximum at JJMC in the afternoon, which normally is observed on glaciers at lower latitudes. Since McCall is at a high elevation and at a high latitude, there is probably insufficient contrast between the temperature of the ambient atmosphere and the glacier surface to produce a maximum in the temperature inversion during day and a katabatic flow (Streten *et al.*, 1974). It is also possible that a valley wind retards the glacier wind during the afternoon (Streten *et al.*, 1974).

Energy balance and specific mass balance at JJMC

For calculating the surface energy balance at JJMC, the radiation components of the energy balance were directly taken from the AWS and the turbulent heat fluxes were calculated from the meteorological measurements, using a bulk method and profile functions of Holtslag and De Bruin (1988). We used a surface roughness length of 2.4 mm estimated by Wendler and Weller (1974) from wind profile measurements on McCall Glacier.

The largest energy flux averaged over the analyzed period is outgoing longwave radiation (–313 W m^{-2}), followed by incoming longwave radiation (284 W m^{-2}). Incoming solar radiation shows the largest day-to-day fluctuations, and its average is 181 Wm^{-2}. Average reflected solar radiation is –71 W m^{-2}, implying that the average albedo is 0.39. The minimum daily mean albedo of the analyzed period is about 0.19, which indicates a value for the ice albedo at JJMC. Increased soot and dust concentrations on the glacier surface can explain the low value for the ice albedo since 2004 was a year with numerous forest fires in Alaska. The turbulent heat fluxes are small and directed towards the surface: the average sensible and latent heat flux is 27 and 5 W m^{-2}, respectively. The sub-surface heat flux is estimated at –5 W m^{-2} (directed away from the surface).

We compared the modeled specific mass balance from the energy balance to data from the sonic height ranger and ablation stakes (Fig. 3). Since the pole of the sonic height ranger melted out halfway the ablation period, there is a data gap in the record and we had to correlate the sonic height ranger data to the stake data. Over the period that ice was melting (15 June to 20 August), the modeled specific mass balance is –2.06 ± 0.18 m w.e (which is the sum of 0.12 m w.e snowfall, 0.003 m w.e. sublimation (deposition), and –2.18 m w.e. melt) while the measured specific mass balance is –1.94 ± 0.09 m w.e. The radiation balance contributes 74% to the energy available for melting.

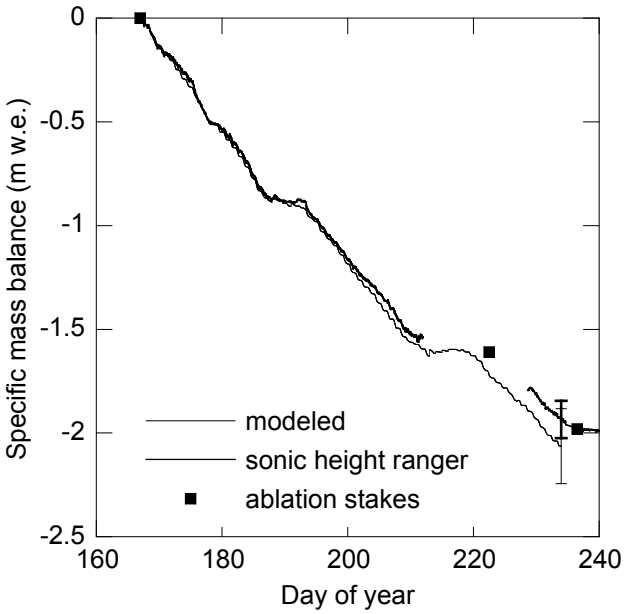

Figure 3. Specific mass balance measured by the sonic height ranger and the ablation stakes. The records start at 15 June and the modeled curve ends at 20 August. For this day, error bars indicate the accuracy of the modeled (thin) and measured (thick) specific mass balance.

References:

Holtslag, A.A.M. and H.A.R. de Bruin (1988). Applied modeling of nighttime surface energy balance over land. Journal of Applied Meteorology, 27, 689–704.

Streten, N.A., N. Ishikawa, and G. Wendler (1974). Some observations of the local wind regime on an Alaskan Arctic Glacier. Arch. Met. Geoph. Biokl., B(22), 337–350.

Wendler, G. and G. Weller (1974). A heat-balance study of McCall Glacier, Brooks Range, Alaska: a contribution to the International Hydrological Decade. Journal of Glaciology, 13(67): 13–26.

http://www.uaf.edu/water/faculty/nolan/glaciers/McCall/index.htm

DERIVING GLACIER MASS BALANCE FROM ELA AND AAR ON STORGLACIÄREN

DIRK-SYTZE KOOTSTRA[1,2], REGINE HOCK[2] AND PETER JANSSON[2]

[1]Department of Physical Geography, Utrecht University
[2]Department of Physical Geography and Quaternary Geology, Stockholm University

Generally good correlations have been found between glacier mass balance and equilibrium line altitude (ELA) or accumulation area ratio (AAR). We investigate this relationship on Storglaciären, Sweden, and test whether the long-term mass balance – ELA or AAR relationships can be determined from transient mass balance measurements throughout just one season as suggested by Dyurgerov (1996). Detailed repeated mass balance measurements were conducted during the melt season 2004 along with observations of snow line retreat. Transient mass balances were related to ELA and AAR revealing good linear correlations, however, the slope of the curves differ significantly from the slopes obtained for the 59-year long mass balance record of Storglaciären (Fig. 1). Hence, it is not possible to substitute the long-term relationship for Storglaciären by the one obtained from the transient measurements in 2004.

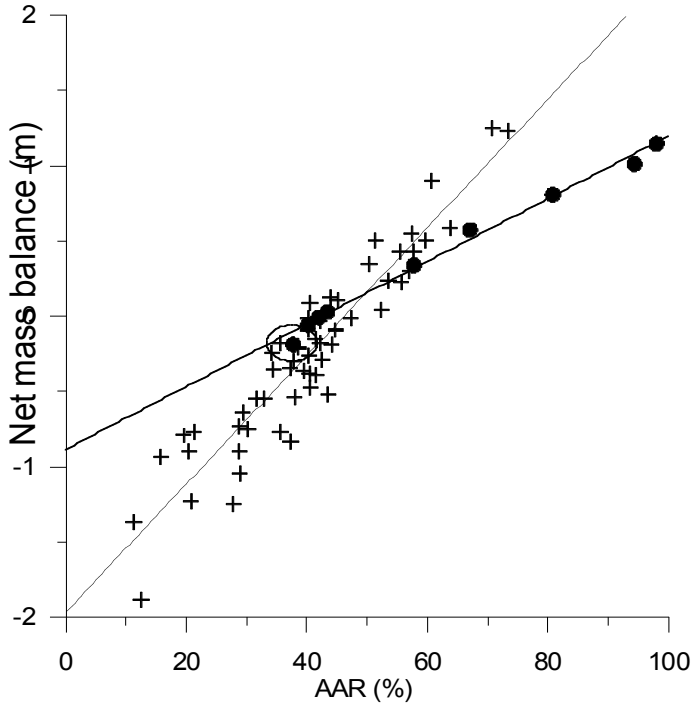

Figure 1. Net mass balance versus AAR for the 59-year mass balance series of Storglaciären (crosses) and the transient mass balances during the 2004 melt season (dots). The circled dot denotes the net balance value for 2004.

Various analyses indicated that this deviation was not caused by errors in the transient mass balance calculations or that 2004 was an abnormal year. There does not seem to be an obvious physical reason for the different relationships. More years should be analyzed since the 2004 mass balance was only slightly negative. It remains open if the relationships agree more closely for more negative years.

References:

Dyurgerov, M., 1996. Substitution of long-term mass balance data by measurements of one summer. *Zeitschrift für Gletscherkunde und Glazialgeologie*, 32, 177-184.

SIMPLE MODELLING OF CALVING GLACIERS

JOHANNES OERLEMANS

Institute for Marine and Atmospheric Research, Utrecht University

Modelling of tidewater glaciers has been very limited (Van der Veen, 1997; Vieli et al., 2001). Here, a simple, highly parameterized model of a tidewater glacier is presented. The mean ice thickness and the ice thickness at the glacier front are parameterized in terms of glacier length and, when the glacier is calving, water depth. A linear relation between calving rate and water depth is used. The change in glacier length is determined by the total change in the mass budget (surface balance and calving flux), but not by the details of the glacier profile and the related velocity field.
The basic equations are:

(mass conservation): $$\frac{\mathrm{d}V}{\mathrm{d}t} = B + F \qquad (1)$$

(ice thickness): $$H_m = \alpha_m \sqrt{L} \qquad (2a)$$

$$H_f = \max\{\alpha_f \sqrt{L};\ -\varepsilon\,(\rho_w / \rho_i)\,d\} \qquad (2b)$$

(calving flux) $$F = \min\{0\,;\,c\,d\,H_f\} \qquad (3)$$

(specific balance) $$B = \beta\,(h_m - E)L \qquad (4)$$

(mean surface height) $$h_m = \frac{b_0 + H_m + b_f + H_f}{2} \qquad (5)$$

In this set of equations V is ice volume, t is time, B is the total surface mass balance, F is the calving flux, H_m is the mean ice thickness, H_f is the ice thickness at the glacier front, α_m and α_f are the corresponding constants of proportionality, L is glacier length, d is water depth at the glacier front, ρ_i and ρ_w are the densities of ice and water, ε is a constant ≥1, c is the calving parameter, β the balance gradient, h_m the mean surface elevation and E the equilibrium-line altitude.
The model described by Eqs. (2)-(5) has been investigated by Oerlemans and Nick (2005). They show that the solution diagram of a tidewater glacier with a submarine shoal (a Gaussian bump on a linearly sloping bed) has two zones of hysteresis: one related to the height – mass balance feedback and one due to the coupling between calving rate and water depth (Fig. 1). Depending on the bed geometry, these two zones are embedded or separated. It should be noted that the formulation for the frontal ice thickness, Eq. (2b), allows a smooth transition from a land-based glacier to a calving glacier.

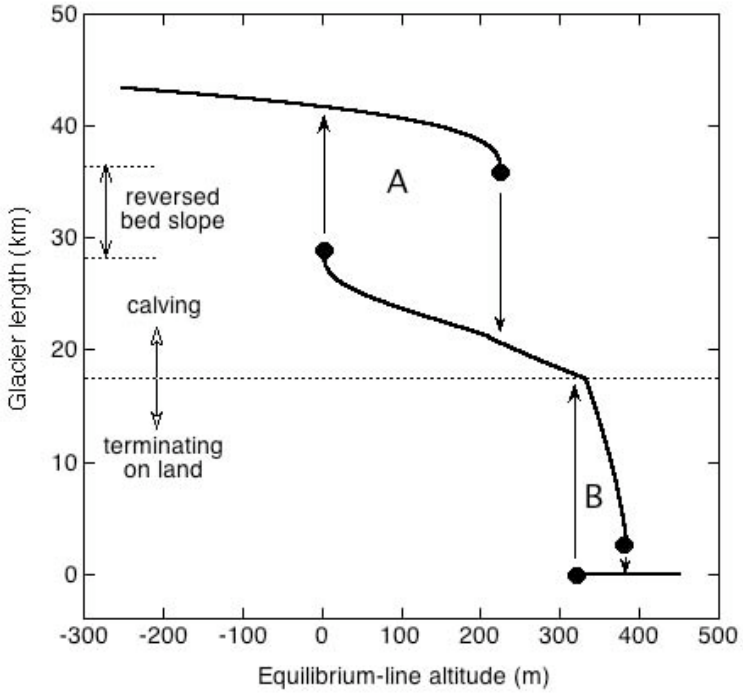

Figure 1. Solution diagram for a tidewater glacier on a bed with a submarine shoal, here located at a distance of about 38 km from the glacier head. Stable equilibrium states and bifurcation points (black dots) are shown as a function of *E*. Two zones of hysteresis are apparent, one associated with the calving process (A) and one due to the height – mass balance feedback (B). Modified from Oerlemans and Nick (2005).

It is possible to couple the simple model of a calving glacier described above to a sedimentation model, implying that the formation of a moraine shoal affects the dynamics of the glacier and vice versa.

The deposition of sediment carried by the ice is a complicated process (e.g. Hunter et al., 1996). Surface debris is partly carried by meltwater streams and channels, findings its way to the bottom of the estuary in one way or another. Another part of the surface debris as well as the englacial debris will be deposited when the icebergs melt, either close to the glacier front or far away. Altogether, it seems reasonable to assume that the deposition rate is largest at the glacier front and drops of smoothly with the distance to the glacier front.

The deposition function *P(x)* used in this study is shown in Fig. 2. The length scale λ determines over what distance along the flowline most of the sediment is deposited a typical value used is 750 m. The deposition rate varies enormously (Hallet et al., 1997). A characteristic value for large tidewater glaciers is 100 $m^2\ a^{-1}$ (this is per unit of glacier width).

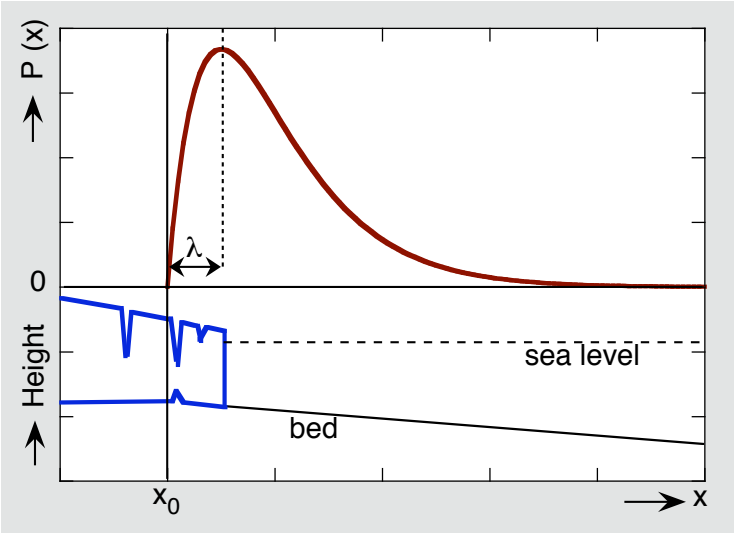

Figure 2. Sediment deposition function used in the calving glacier model.

A number of calculations was carried out for a typical geometry of a small-slope tidewater glacier. The climatic forcing was prescribed as a period movement of the equilibrium line.

An example is shown in Fig. 3. The initial condition is L=0 and then a glacier starts to form because the equilibrium line is lowering (the highest point of the bed is 200 m above sea level and it drops of linearly with a slope of 0.01). After 2000 years of integration, when the equilibrium line attains its minimum value, glacier length changes very little for a long time. The total surface balance decreases because the equilibrium line goes up, and the calving rate becomes smaller because the water depth decreases. During the period 2000–4000 years these fluxes are reduced by 50%, while the glacier length shows little change. Finally, at t=4070 the system becomes unstable and the glacier withdraws from the morainic shoal. Because the water depth at the glacier front then increases rapidly, the calving flux doubles within 100 years and glacier retreat accelerates.

The corresponding evolution of the bed is shown in Fig. 4. Because the glacier grows rapidly into the estuary, the sediment is spread over a large area and the result is a small increase in the bed elevation over a large distance. When the advance of the glacier front decelerates the building of a moraine shoal starts. Shortly before the retreat of the glacier starts the moraine shoal is about 100 m high and a few km wide, and changes little afterwards.

It can be concluded that the change of the glacier bed due to sediment deposition has a profound influence on the behavior of the tidewater glacier. The formation of a moraine shoal tends to lock the position of the glacier front. Because the bed slope in front of the shoal is steep, and gets steeper all the time, only a very small adjustment of the glacier length is needed to change the calving flux in such a way that it balances the surface mass balance. However, in the case of a rising equilibrium line, ultimately the surface mass balance becomes so small that the

total mass budget becomes negative. At that point the decay has to set in and runaway retreat is inevitable.
The combined glacier-sediment model presented in this paper is about the simplest that can be constructed. Yet, it exhibits interesting dynamic behavior. The model is able to simulate a typical advance-retreat cycle for a tidewater glacier without subtle tuning or numerical tricks.

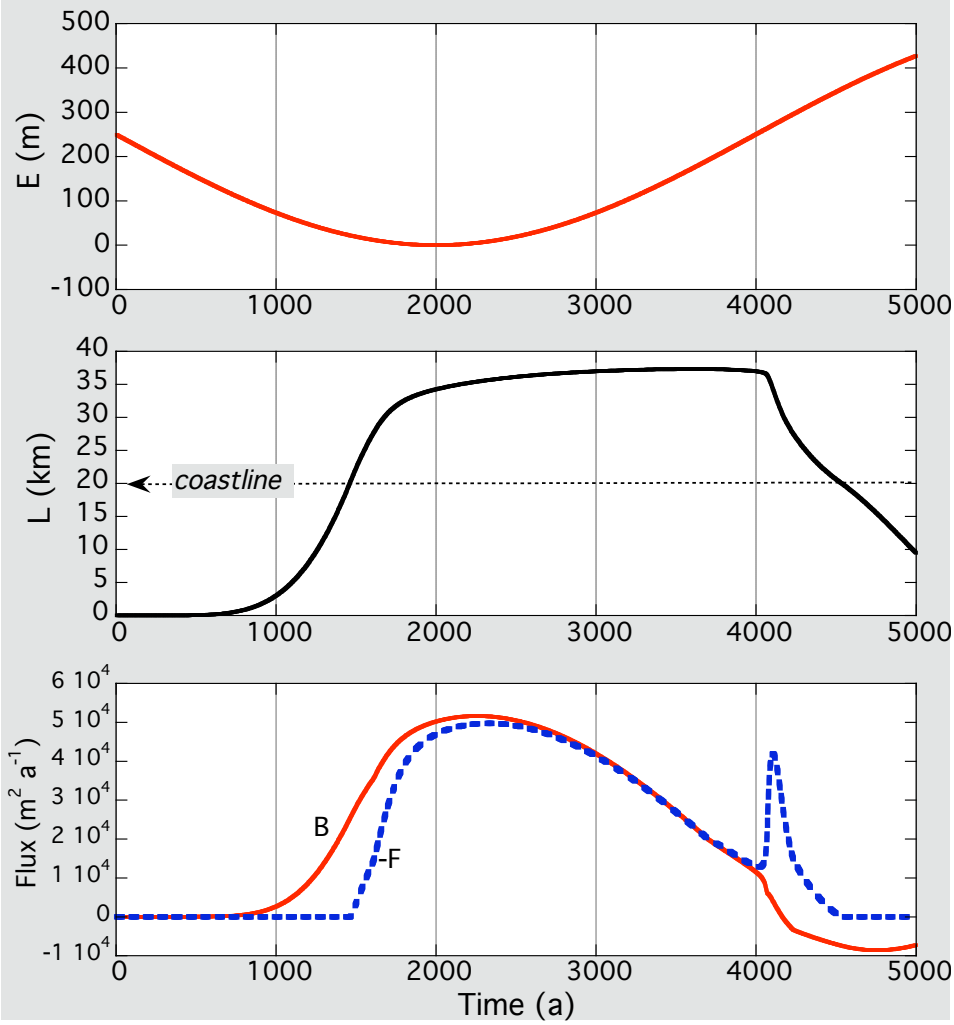

Figure 3. The response of the coupled glacier-sediment model to periodic forcing of the equilibrium line (upper graph). The glacier length *L* is shown in the middle. the lower panel shows the components of the mass budget: the total surface mass balance *B* and the calving flux *F*.

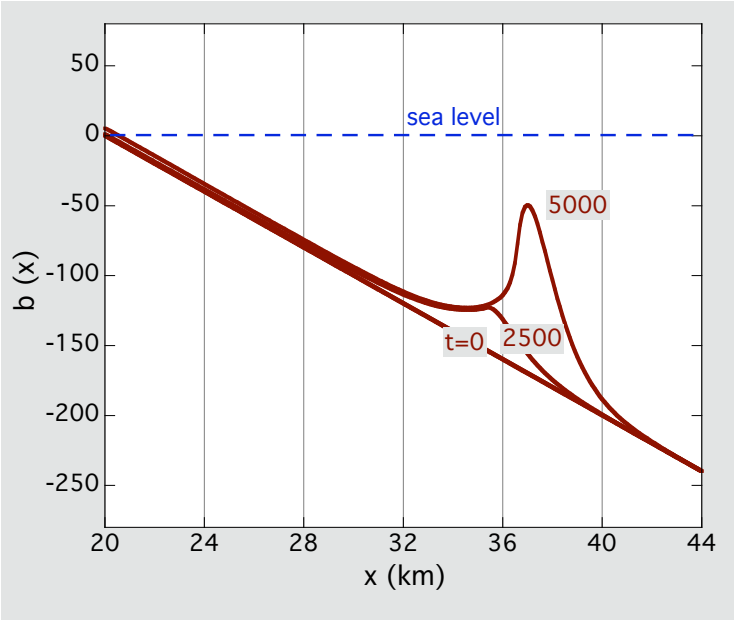

Figure 4. Evolution of the bed profile for the reference calculation with periodic forcing. Labels refer to time in a.

The next step obviously is to try to apply the model to real glaciers. This will require some modifications. Rather than assuming a constant width, the model should then describe laterally-averaged conditions in which convergence or divergence of the flow is taken into account. It will be interesting to see if it is possible to simulate the late-holocene history of some well documented tidewater glaciers.

References

Hallet, B., Hunter, L., and Bogen, J., 1996. Rates of erosion and sediment evacuation by glaciers: A review of field data and their implications. Glob. Planet. Change 12, 213-235.

Hunter, L. E., Powell, R. D., and Lawson, D. E. 1996. Morainal-bank sediment budgets and their influence on the stability of tidewater termini of valley glaciers entering Glacier Bay, Alaska, U.S.A., Ann. Glaciol. 22, 211-216.

Hunter, L. E., Powell, R. D., and Lawson, D. E. 1996b. Flux of debris transported by ice at three Alaskan tidewater glaciers. J. Glaciol 42(140), 123-135.

Oerlemans, J., and Nick. F. M., 2005. A minimal model of a calving glacier. Ann. Glaciol. 42, in press.

Van der Veen, C. J. (ed.), 1997. Calving Glaciers: Report of a Workshop, February 28 - March 2, 1997, Byrd Polar Research Center Report no. 5, Ohio State University (Columbus, Ohio, U.S.A.), 194 pp.

Vieli, A., Funk, M., and Blatter, H., 2001. Flow dynamics of tidewater glaciers: a numerical modelling approach. J. Glaciol. 47(159), 595-606.

ON ELEVATION CHANGES OF SVALBARD GLACIERS

J.O. HAGEN, T. EIKEN AND K. MELVOLD

Department of Geosciences, Faculty of Mathematics and Natural Sciences, University of Oslo, P.O. Box 1047 Blindern, 0316 Oslo, Norway. E-mail: j.o.m.hagen@geo.uio.no

Recently, ground based GPS measurements, airborne and satellite borne laser and radar altimeters have been used for mapping geometry changes on glaciers, ice caps and ice sheets. Geometry changes given as longitudinal elevation profiles have then been used in mass balance estimates by input to digital terrain models to calculate the volume changes (mass balance). However, the geometry of glaciers is affected by both the mass balance and the dynamics and it is therefore not straightforward to interpret elevation changes.

In Svalbard several glaciers have been measured by repeated elevation profiles both by ground-based GPS measurements [1] and by airborne laser altimetry [2], [3].

We have shown by three examples from Spitsbergen glaciers that different dynamics of the glaciers can give quite different elevation profile changes independent of the mass balance [1]. Surging glaciers are frequent in Svalbard and during the quiescent period the glacier will shrink in the lower part and be thickening in the upper part independent of climate or mass balance. This must be taken into consideration when elevation profiles are used in mass balance discussions.

In addition to our ground-based GPS measurements repeated laser profiles were carried out by NASA in 1996 and 2002 [2], see Fig 1. The NASA results showed in general a thinning of the glaciers, mostly in southern Spitsbergen, and less in northern and eastern ice masses. On a few spots the GPS and laser profiles are overlapping and could be compared. On the glacier Kongsvegen in north-west Spitsbergen our GPS data and the laser profiles showed the same trend with thickening in upper part and lowering of the surface in the ablation area. This should indicate that both data sets give reliable data, at least in the general pattern. However, the numbers are not exactly the same.

On Austfonna ice cap the NASA data indicate a clear thickening of the upper central part of the ice cap and a peripheral thinning [3]. The net balance derived form our shallow cores indicate, however, a balance close to zero [4], and the GPS profiles indicate less pronounced thickening and less thinning. The GPS-profiles also show that different parts of the ice cap can develop differently. In two profiles taken from the summit, one to the North-West and the other to the South-West (Etonbreen) showed a different trend with thickening towards the lower part in North-West and thinning in South-West, Fig. 2. The ground based differential GPS profiles across the ice cap have been done in 1999 and 2004. They are not overlapping the NASA profiles, but in parts the profiles are crossing. The next step in these analyses will be to compare the data sets for crossing points in order to see if we can calibrate the two data sets together.

It is, however, clear from all the different data sets that we need extensive data to be able to make reliable assessments of mass balance, covering different types and sizes of glaciers in which the dynamic effect must be considered.

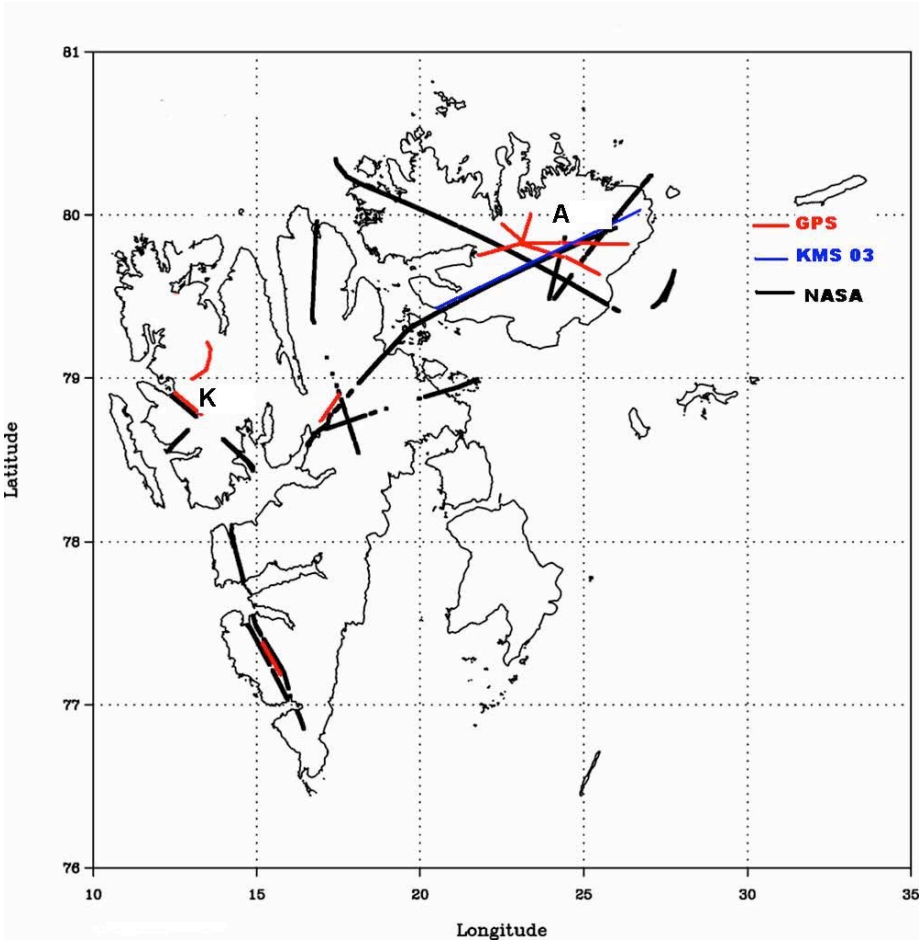

Figure 1. Location of repeated elevation profiles on Svalbard glaciers. K – Kongsvegen, A - Austfonna

References

[1] Hagen, J. O., T. Eiken, J. Kohler, K. Melvold, in print: Geometry changes on Svalbard glaciers – mass balance or dynamic response? Annals of Glaciology 42

[2] Bamber, J. L., W. Krabill, V. Raper and J. A. Dowdeswell, in print: Interpretation of Elevation Changes on Svalbard Glaciers and Ice Caps from Airborne Lidar Data. Annals of Glaciology 42

[3] Bamber, J. L., W. Krabill, V. Raper and J. A. Dowdeswell (2004). Anomalous recent growth of part of a large Arctic ice cap: Austfonna, Svalbard. Geophys. Res. Lett. 31(12): doi:10.1029/2004GL019667.

[4] Hagen, J.O., K. Melvold, F. Pinglot and J. A. Dowdeswell. 2003a. On the net mass balance of the glaciers and ice caps in Svalbard, Norwegian Arctic. Arct. Antarct. Alp. Res., 35(2), 264-270.

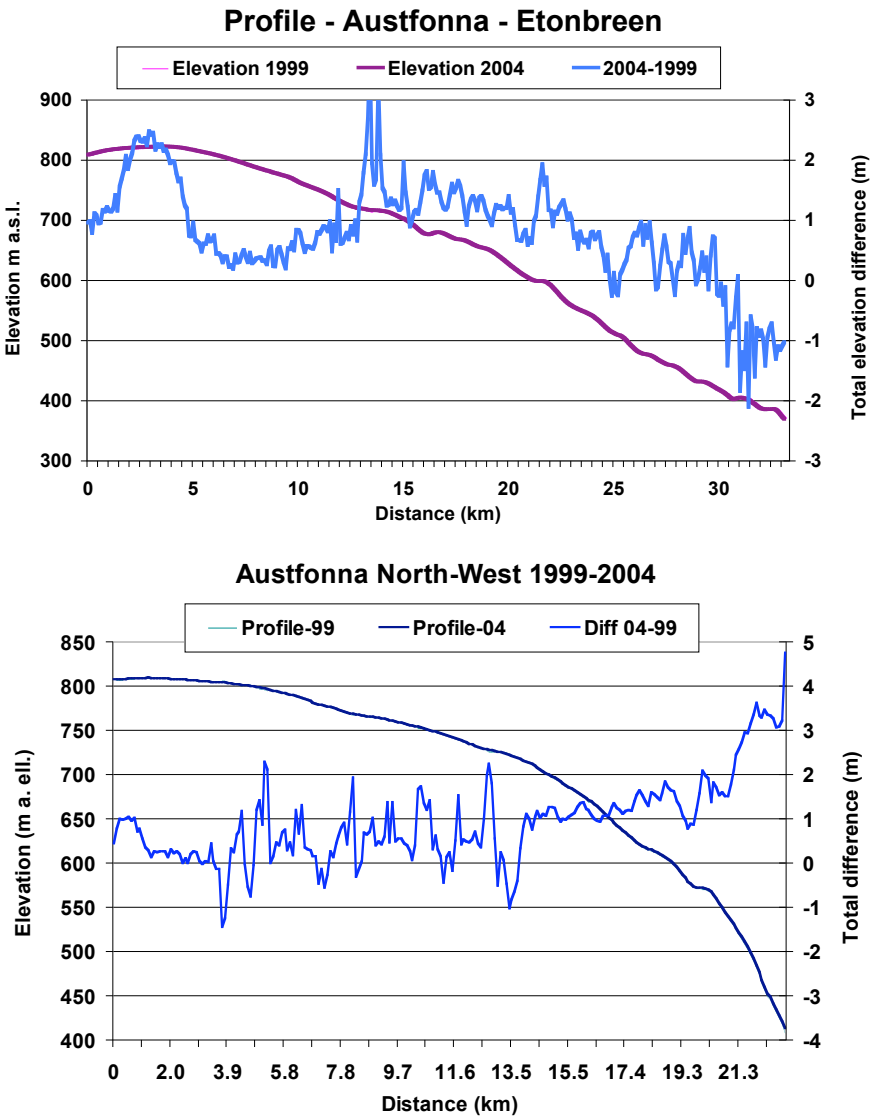

Figure 2. Two profiles on Austfonna showing a different trend towards the edge of the ice cap.

AUTOMATIC WEATHER STATIONS IN THE ABLATION ZONE OF THE WEST GREENLAND ICE SHEET

MICHIEL VAN DEN BROEKE, PAUL SMEETS, WIM BOOT, JOHANNES OERLEMANS, WOUTER GREUELL AND RODERIK VAN DE WAL

Utrecht University, Institute for Marine and Atmospheric Research (UU/IMAU)

Background

In 1990 and 1991, the Ice and Climate research group of UU/IMAU started its experimental Greenland research by performing two detailed meteorological experiments in the ablation zone of the west Greenland ice sheet near Kangerlussuaq. The experiments consisted of several multi-level automatic meteorological stations on the tundra and on the ice (Fig. 1). A base camp was established at the ice sheet edge, where a cabled balloon was operated to gauge the lowest 1000 m of the atmosphere. In 1991, the Free University of Amsterdam performed turbulence measurements and a 30 m profile tower at 1500 m asl (Oerlemans and Vugts, 1993). During these summer campaigns, weekly mass balance measurements were performed to track seasonal melting. The mass balance measurements range in elevation from the ice edge (360 m asl) to the equilibrium line at approximately 1500 m asl, and are indicated by flags in Fig. 1.

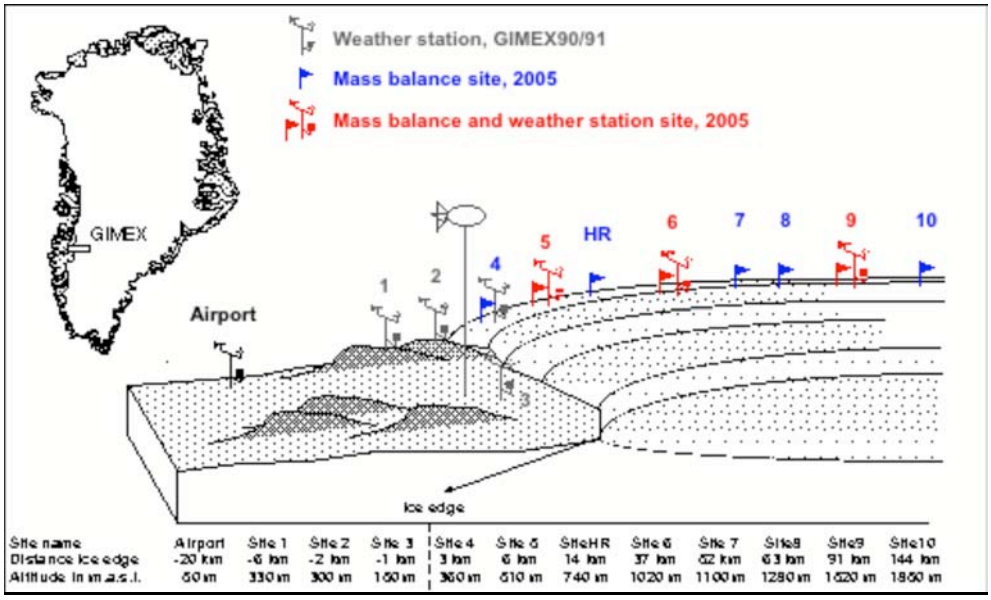

Figure 1. Experimental set-up of GIMEX-90/91 campaigns and locations of mass balance and AWS sites that have remained active (situation of January 2005).

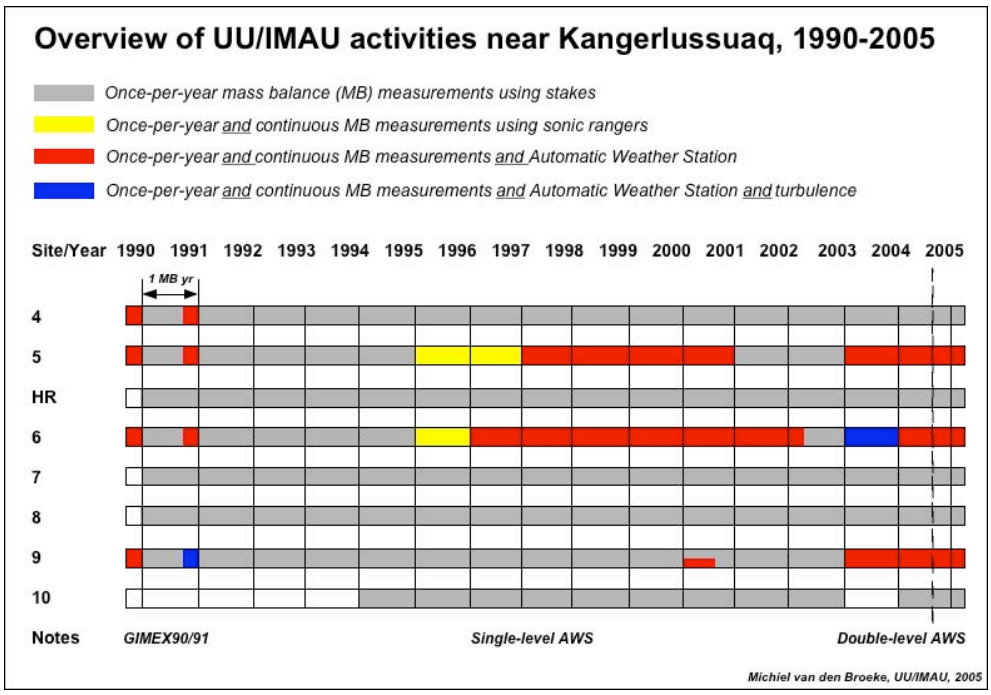

Figure 2. Overview of UU/IMAU activities in the area of Kangerlussuaq, 1990-2005.

These mass balance measurements have been continued up to the present day (Fig. 2), although at lower temporal resolution, namely once per year (at the end of August). In August 1994, the mass balance transect was extended to 1850 m asl to include a site in the accumulation zone.

In August 1995, sonic height rangers were deployed at sites 5 and 6 to measure ablation and accumulation continuously. The Kangerlussuaq mass balance series now covers 13 seasons and is the longest of its kind in Greenland (Van de Wal et al., 1996; Greuell et al., 2001).

In the early 1990s, IMAU technicians started developing automatic weather stations (AWS) for use in the ablation zone of ice sheets and glaciers. A stiff construction was envisaged that would be able to stand freely on the ablating ice surface, without tipping over under strong wind conditions and without tilting too much. The final result consisted of an aluminum mast on four legs, interconnected with steel guy wires, with pins at the end for better grip. This design proved to be very reliable with only limited tilt even at places with several meters of annual ablation; it has been applied to glaciers in Iceland, Norway and the Alps and on blue ice areas in Antarctica. In Greenland, the first year-round AWS data were collected onwards from August 1996 (Fig. 2). Several years of successful AWS operation followed at sites 5 and 6. Unfortunately, because the operation and maintenance of the AWS was not funded from a dedicated project, maintenance of the AWS became problematic which resulted in data quality loss from 2001 onwards (Fig. 2).

The new AWS network, August 2003

In 2003 it was decided that reliable, continuous meteorological data were required for better interpretation of spatial and temporal mass balance variability. Moreover, regional climate models also urgently require need validation data from the ice sheet and improved parameterizations of surface processes.

With funds from COACH (Cooperation in Oceanographic and Atmospheric Research) and NAP (Netherlands Arctic Program), new stations were built and installed in 2003 at sites 5, 6 and 9 by IMAU technicians. Moreover, a prototype eddy correlation station with dedicated power supply was installed at site 6. Fig. 3 shows the experimental setup at site 6. The first year of data collection from the new network (August 2003-August 2004) revealed some imperfections in sensor performance, but overall results are very exciting: for the first time, year-round eddy correlation observations had been collected in the Greenland ablation zone for both heat and moisture, while the vulnerable thermocouple had survived a full year of observations unharmed.

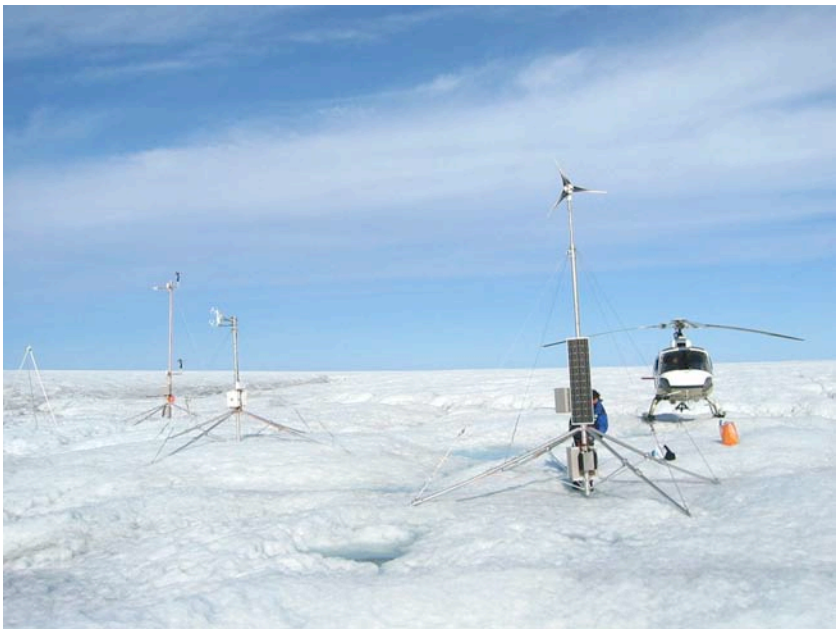

Figure 3. Site 6, August 2003. From right to left: wind generator and solar panel for eddy correlation station, the eddy correlation station, the AWS and the sonic height ranger.

The data presently being analyzed are providing us with insight about e.g. radiation errors of unventilated temperature huts, the validity of flux-profile relations, temporal variability of surface roughness for momentum (smoother in winter than in summer), validity of the expressions relating surface roughness for heat and moisture to that of momentum etc. The eddy correlation station was removed in

August 2004 to assess its performance and to further improve its design. Based on the present achievements, it is expected that similar eddy correlation stations will be installed at other Greenland as well as Antarctic sites, pending funding decisions. To conclude, the revitalized AWS network is likely to produce data useful for the interpretation of mass balance observations, the validation regional climate models and development of improved parameterizations for surface exchange of momentum, heat and moisture.

Useful references

Abdalati, W., and K. Steffen, 2001: Greenland ice sheet melt extent: 1979-1999, Journal of Geophysical Research 106, 33,983-33,988.

Ambach, W., 1977: Untersuchungen zum energieumsatz in der ablationszone des Grönländische inlandeises, Expedition Glaciologique Internationale au Groenland 4, No. 5, Bianco Lunos Bogtrykkeri A/S, København, pp 63.

Box, J. E. and A. Rinke, 2003: Evaluation of Greenland ice sheet surface climate in the HIRHAM regional climate model, Journal of Climate 16, 1,302-1,319.

Cassano, J. J., J. E. Box, D. H. Bromwich, L. Li, S. Konrad, 2001: Evaluation of Polar MM5 simulations of Greenland's atmospheric circulation, Journal of Geophysical Research 106, 33,867-33,890.

Church, J.A., J.M. Gregory, P. Huybrechts, 2001: Changes in sea-level, in IPCC Third Scientific Assessment of Climate Change, edited by J.T. Houghton, and D. Yihui, pp. 640-693, CUP, Cambridge.

Comiso, J.C., 2003: Warming trends in the Arctic from clear sky satellite observations, J. Climate 16, 3498-3510.

Fettweis, X., H. Gallée, J.-P. van Ypersele, 2004: Surface mass balance of the Greenland ice sheet simulated with a coupled atmosphere-snow regional model, Climate Dynamics, in press.

Fichefet, T., C. Poncin, H. Goosse, P. Huybrechts, I. Janssens and H. Le Treut, 2003: Implications of changes in freshwater flux from the Greenland ice sheet for the climate of the 21st century, Geophysical Research Letters 30, doi: 10.129/2003GL017826.

Gallée, H., O. F. de Ghélin and M. R. van den Broeke, 1995: Simulation of atmospheric circulation during the GIMEX-91 experiment using a meso-g primitive equations model, J. Climate 8, 2843-2859.

Greuell, W. and W. H. Knap, 2000: Remote sensing of the albedo and detection of the slush line on the Greenland ice sheet, J. Geophys. Res., 105 15, 567-15,576.

Greuell, W., B. Denby, R. S. W. van de Wal and J. Oerlemans, 2001: 10 years of mass balance measurements along a transect near Kangerlussuaq, central West Greenland, J. Glaciol. 156, 157-158.

Heinemann, G., 1999: The KABEG '97 field experiment: an aircraft-based study of katabatic wind dynamics over the Greenland ice sheet, Bound. Layer Meteorol. 93, 75-116.

Huybrechts, P., I. Janssens, C. Poncin and T. Fichefet, 2002: The response of the Greenland ice sheet to climate changes in the 21st century by interactive coupling of an AOGCM with a thermomechanical ice sheet model, Annals of Glaciology 35, 409-415.

Oerlemans, J. and H. F. Vugts, 1993: A meteorological experiment in the melting zone of the Greenland ice sheet, Bulletin of the American Meteorological Society 74, 355-365.

Rahmstorf, S., 1995: Bifurcations of the Atlantic Thermohaline Circulation in Response to Changes in the Hydrological Cycle, Nature 378, 145-149.

Steffen, K. and J. Box, 2001: Surface climatology of the Greenland ice sheet: Greenland Climate Network 1995-1999, Journal of Geophysical Research 106(D24), 33,951-33,964.

Van den Broeke, M. R., P. G. Duynkerke and J. Oerlemans, 1994: The observed katabatic flow at the edge of the Greenland ice sheet during GIMEX-91, Global Planet. Change 9, 3-15.

Van den Broeke, M. R., P. G. Duynkerke and E. A. C. Henneken, 1994: Heat, momentum and moisture budgets of the katabatic layer over the melting zone of the west Greenland ice sheet, Boundary-Layer Meteorol. 71, 393-413.

Van den Broeke, M. R., and H. Gallée, 1996: Observation and simulation of barrier winds at the western margin of the Greenland ice sheet, Quart. J. R. Met. Soc. 122, 1365-1383.

Van de Wal, R. S. W., M. Wild and J. De Wolde, 2001: Short-term volume changes of the Greenland ice sheet in response to doubled CO2 conditions, Tellus 53(B), 94-102.

Wild, M., P. Calanca, S. C. Scherrer and A. Ohmura, 2003: Effects of polar ice sheets on global sea level in high-resolution greenhouse scenarios, Journal of Geophysical Research 108(D5) 4165, doi:10.10129/2002JD002451.

Zwally, H.J., W. Abdalati, T. Herring, K. Larson, J. Saba, and K. Steffen, 2002: Surface melt-induced acceleration of Greenland ice-sheet flow, Science 297, 218-220.

GLACIER VELOCITIES IN THE CANADIAN HIGH ARCTIC FROM RADARSAT-1 SPECKLE TRACKING

N. H. SHORT[1] AND A. L. GRAY[2]

[1] Noetix Research Inc., 265 Carling Ave. suite 403, Ottawa, ON, K1S 2E1, Canada; naomi.short@ccrs.nrcan.gc.ca (on contract to the Canada Centre for Remote Sensing)
[2] Canada Centre for Remote Sensing, 588 Booth St., Ottawa, ON, K1A 0E4, Canada; e-mail: laurence.gray@ccrs.nrcan.gc.ca

The surface velocities of 11 glaciers from the Queen Elizabeth Islands of the Canadian high Arctic have been monitored between 2000 and 2004 using RADARSAT-1 data and the speckle tracking technique, creating a broad overview of glacier dynamics in this region. Where ice thickness measurements are available they have been combined with the velocity results to estimate calving rates. In a few cases they have also been used to derive theoretical balance velocities to compare with the velocity measurements.

RADARSAT-1 Fine Mode data are optimal for the high relief and relatively narrow glaciers of the Canadian Arctic and most data sets were obtained at this ~9 m resolution. Only large glaciers were selected for study since the speckle tracking technique dictates that sites should be > 1.5 km in width. Fig. 1 shows the locations of the studied glaciers. The speckle tracking velocity measurements are thought to be accurate to ±14 m a^{-1}, with additional errors over floating ice tongues depending on the tides.

The results show that the flow of large outlet glaciers in the Canadian Arctic can be fast and variable. Speeds of several hundreds of metres a year are common and flow rates of ~ 1 km a^{-1} are attainable under surge conditions. At any one time several glaciers appear to be actively surging and active phases of 5-9 years minimum have been observed. Other glaciers demonstrate significant short-medium term variations in flow rates even though they are not considered to be surge type, perhaps suggesting that pulses and cycles other than full surges are an important part of Arctic ice dynamics. Some example results are shown in Figures 2-6.

These observations of local, short-medium term flow instabilities have implications for the interpretation of measured ice thickness and surface height changes, particularly in the field of detecting cryospheric climate induced change. The identification of 'control' regions, those unaffected by short-medium term flow instabilities might be a strategy for finding reliable evidence of long-term climate forcing in the Arctic.

It appears that speckle tracking results can make useful contributions to the calculation of calving rates (see Table 1), more ice thickness measurements are needed to expand this application. To perform reliable comparisons with balance velocities, finer resolution SAR data and more measurements of ice thickness and ablation rates are needed.

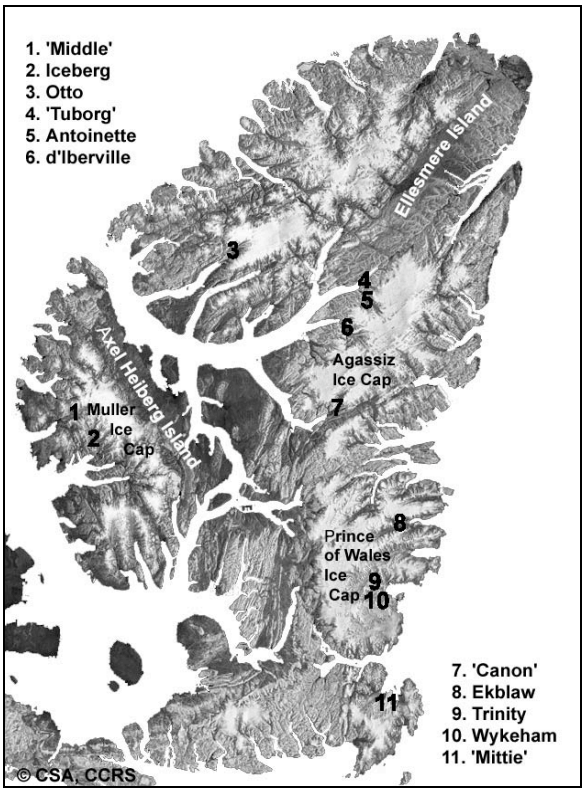

Figure 1. Axel Heiberg and Ellesmere Islands with the locations of the studied glaciers. Unofficial names are denoted with quotes. The background is a mosaic of RADARSAT-1 ScanSAR imagery collected in January and February 1998.

Table 1. Calving rates for select glaciers

Glacier and year	**Terminus width (km)**	**Centre line thickness* (m)**	**Mean velocity (m a^{-1})**	**Retreat or advance (km^3 a^{-1})**	**Calving rate ‡ (km^3 a^{-1})**
Otto 2002 2003 2004	3.5	120	650 875 800	0.15 advance no change 0.27 retreat	0.12 ± 0.03 0.37 ± 0.09 0.61 ± 0.15
Wykeham 2004	3.0	225	370 †	0.03 advance	0.22 ± 0.05
Ekblaw 2003	2.1	400	350 †	no change	0.29 ± 0.07

* From Gogenini (1995).

† Velocity estimates have been adjusted for tidal effects

‡ Overall errors of 25% are quoted to accommodate the spatial limitations of the ice thickness measurements and high velocity errors due to degradation of speckle tracking to feature tracking.

References

Gogenini, P., 1995. ftp://tornado.rsl.ukans.edu/pub/greenland/1995/pdf/may26_95.pdf (Accessed May 2004)

Hattersley-Smith, G., Fuzesy, A. and Evans, S. 1969. Glacier depths in northern Ellesmere Island: airborne radio echo sounding in 1966. Defence Research Board, Ottawa. Report Geophysics Hazen 36, DREO Technical Note No. 69-6.

Some example results

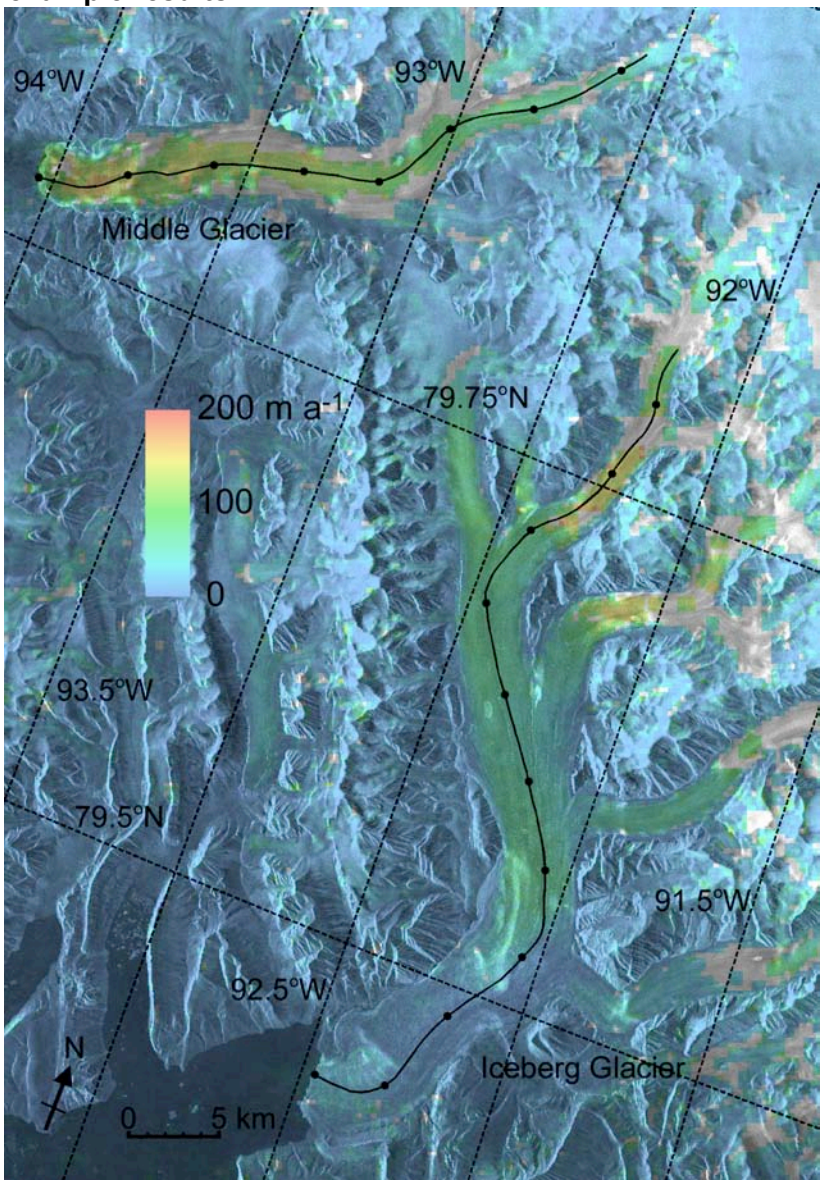

Figure 2. 2004 surface velocities of Middle and Iceberg glaciers. Profiles are marked at 5 km intervals.

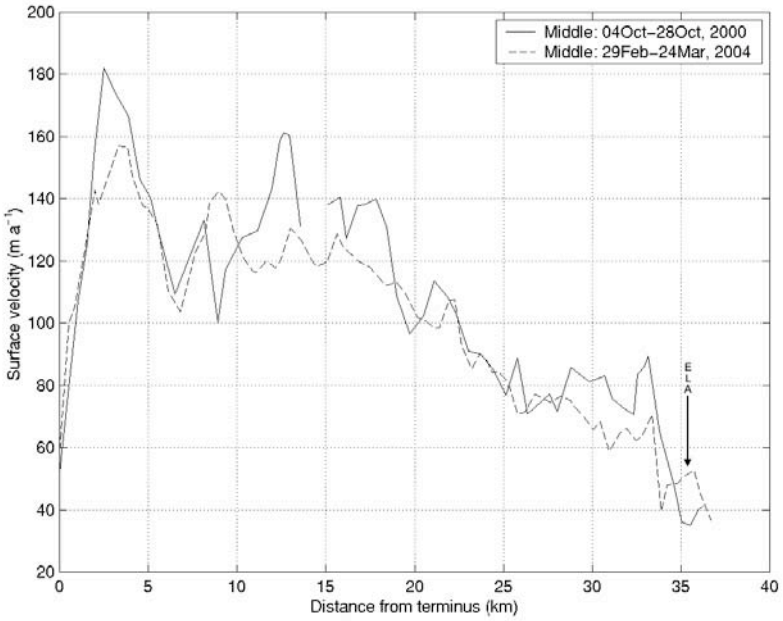

Figure 3. Surface velocity profiles of Middle Glacier in 2000 and 2004. ELA indicates approximate equilibrium line altitude.

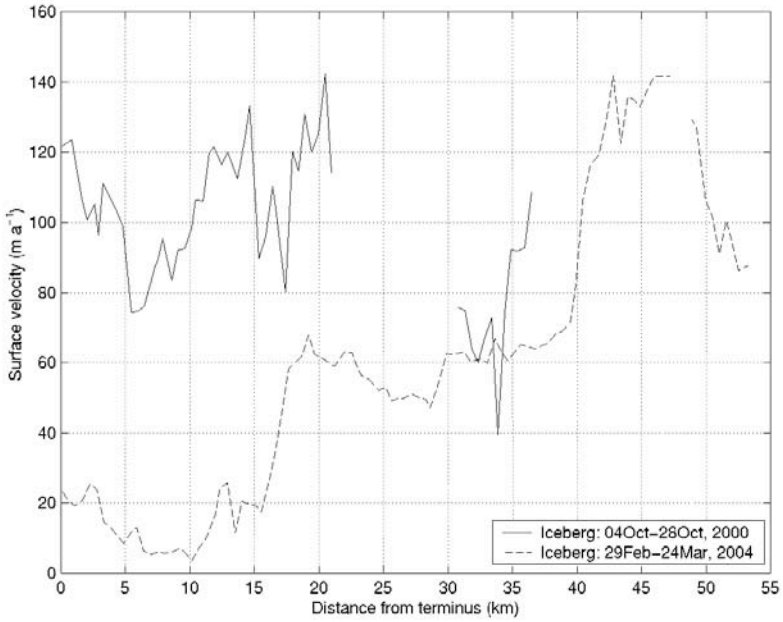

Figure 4. Velocity profiles of Iceberg Glacier in 2000 and 2004.

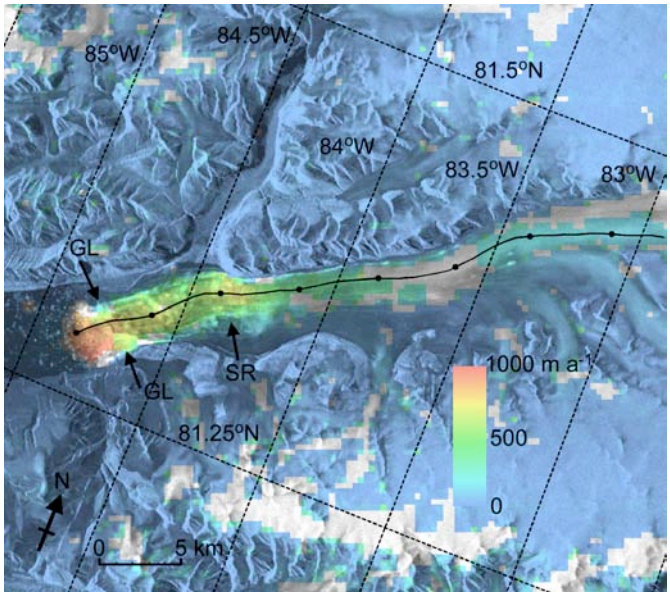

Figure 5. Surface velocities of Otto Glacier in 2003 with profile location marked at 5 km intervals. SR indicates location of subglacial ridge and GL the grounding line, both after Hattersley-Smith et al., (1969).

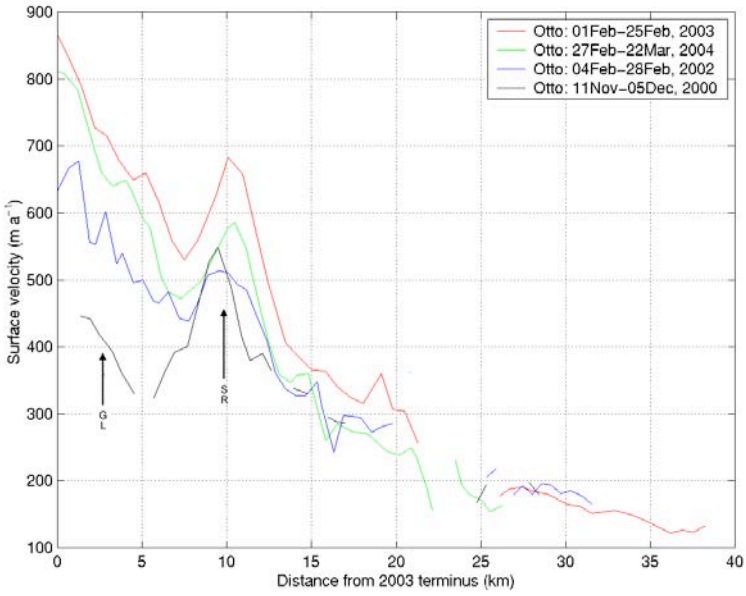

Figure 6. Surface velocity profiles of Otto Glacier in 2000, 2002, 2003 and 2004. Grounding line (GL) and subglacial ridge (SR) locations taken from Hattersley-Smith et al., (1969).

USE OF TIME-LAPSE CAMERAS ON AUTOMATIC WEATHER STATIONS

MATT NOLAN

UAF, Fairbanks, Alaska

Time-lapse cameras have the ability to substantially improve our understanding of glacier-climate interactions, particularly in association with automatic weather stations. A fundamental problem with automatic weather stations (AWSs) is inherent to their nature -- they are located in remote locations with little oversight by their creators. Often problems associated with riming, blowing snow, and sensor tilting go undetected for long-periods of time and may never be detected as they are sometimes self-correcting. In such cases, the digital data recorded for a particular sensor may be well outside of the normal accuracy bounds yet the instrument may still be functioning perfectly. Here we present several examples of how we are starting to use time-lapse cameras to improve our understanding of glacier-climate interactions on McCall Glacier, Alaska.

We installed a time-lapse camera near an AWS was placed in the firn. This station began tilting immediately after it was left for the summer. The tilt was slow, but detectable using the camera. The tilt most strongly affected the sonic ranger attached to the station, which was intended to measure changes in snow depth. Comparison of the sonic ranger data with changes in snow depth measured from the camera's images of a segmented snow-stake (a "snow ruler") showed that the sonic ranger was in error by more than 0.50 m by the end of the summer.

We installed a time-lapse camera on an AWS on a mountain top to watch snow melt progress through summer in the ablation zone, where another AWS was located on the ice. This camera showed not only snow line progression, but also late-summer snow falls and the patterns of subsequent wind scour that moved this snow in a discontinuous pattern off the surface. These images are complementary to the AWS data measured on the ice surface, which only represent point values of snow depths, albedo, and wind speeds.

We installed a camera a few meters from this same AWS in the ablation are to watch how it functioned throughout the summer. This station was a 'floating' station, which was not directly attached to the ice surface. Rather, the station is internally stable and rigid, and allowed to ride the melting ice surface downward. The time-lapse camera showed that this new station design was reliably stable to within the resolution of the camera, with no major tilting events observed. The images also showed the progression of snow melt past the station (complementary to the one installed higher up on the mountain) to show the local conditions which the four component radiometer was measuring. Here a small stream formed temporarily beneath the radiometer and underneath the station, likely as a result of surface disturbance during station installation in spring. This stream did not continue running once snow melt was complete and it appeared that the surface measured there was representative of the surrounding surface.

Finally, we present a time-series of images acquired every minute over a single sunny day. These images show the temporal patterns of shadows caused by the

steep valley walls and the Arctic sun's travel around the sky. We used this time-series to validate a shading model used in spatially-distributed mass balance modeling. This model uses a digital elevation model of the area and the sun's geometry throughout the day to predict which parts of the glacier will be shaded. Movies were made of both the time-lapse camera output and the model, at the same time-step and approximately the same vantage point. These movies, run side-by-side, show that the model is representing the actual shading quite well, though artifacts in the DEM are clearly present and introduce noise.

In summary, we believe that time-lapse cameras make valuable additions to standard AWS instrumentation. Further technological developments are required, however, as currently choices are limited for off-the-shelf packages for time-lapse cameras that can work reliably in cold, harsh weather on low power in bright sun. The off-the-shelf camera systems we used met these requirements fine, but suffered from having sub-megapixel resolution which limits their applicability and visual appeal.

RECONSTRUCTION OF PAST ACCUMULATION RATES IN AN ALPINE FIRN REGION: FIESCHERHORN, SWISS ALPS

AUREL SCHWERZMANN[1,2], MARTIN FUNK[1], HEINZ BLATTER[2], MARTIN LÜTHI[1,3], MARGIT SCHWIKOWSKI[4], ANNE PALMER[4,5]

[1]Laboratory for Hydraulics, Hydrology und Glaciology, ETH-Zentrum, CH-8092 Zürich, Switzerland
[2]Institute for Atmospheric and Climate Science, ETH-Zentrum, CH-8092 Zürich, Switzerland
[3]present adress: University of Alaska, Fairbanks, Alaska
[4]Paul Scherrer Institute, CH-5232 Villigen, Switzerland (also at University of Berne)
[5]present adress: University of Tasmania, Hobart, Tasmania

Firn and ice layers in polar and high mountain ice masses constitute valuable archives of past climates and the history of chemical composition of the atmosphere. A new ice core was drilled on Fiescherhorn Glacier in December 2002 in the context of the project VITA (Varves, Ice cores and Tree rings: Archives with annual resolution) of the Swiss National Center of Competence in Research (NCCR Climate). The project VITA explores a combination of different types of natural archives that are able to record environmental and climatic changes on the highest possible time scale. One of the purposes of the ice core drilling was the reconstruction of past annual acumulation. In this work we present a method to determine the thinning of annual firn layers with depth.

The study site is located in the accumulation area of the Fiescherhorn glacier in the Swiss Alps on a plateau of about 0.5 km^2 between the mountains Grossfiescherhorn (4049 m asl) and Hinterfiescherhorn (4025 m asl). The plateau has a mean elevation of about 3900 m asl and slopes 12% towards the northeast. The ice core drilled in December 2002 (Hole B02) reached the bed of the ice at a depth of 150 m. It is situated at an elevation of 3900 m asl in the middle of the accumulation plateau from Fiescherhorn glacier. At this altitude, melt may occur in warm summers and can also be caused by melt due to albedo decrease by dust layers (Palmer and others, 2004). Melt water percolation may not only diffuse chemical tracer species but the formation of ice lenses through refreezing of melt water also results in a complex density profile.

In one year, a snow layer of thickness h_A and density ρ_A is accumulating at surface point A. Covered by new layers, this selected layer thins to h_B and density ρ_B as it moves to greater depth at point B. From ice core analysis, only today's observed annual layer thicknesses h_B are known. To reconstruct the original layer thickness h_A of the same layer at the time of its accumulation at the surface, today's observed thickness h_B must be corrected by a factor k, which can be interpreted as a “geometrical thinning factor”:

$$k = \frac{h_\mathrm{A}}{h_\mathrm{B}} \qquad (1)$$

Small variations in accumulation rate at the surface, such as variations in surface snow density or submergence velocity, do not change the mean vertical velocity at

depth. Such irregularities can be expected to diminish with depth (Nye 1975) which leads to a steady state long-term averaged vertical velocity.
Relaxation of the restrictive conditions of steady state to the assumption that only the density field is in steady state and only a function of depth below ice surface (Sorge's Law: see e.g. Bader, 1954) requires either additional measurements or an additional assumption of ice mass continuity. This case may be generalized to a 3-dimensional field such as a borehole in a sloping region, because the integrated thinning does not depend on the particle path, but only on the starting point at the surface and the point of the ice sample in the borehole. On the other hand, this requires some information on the position where the corresponding ice samples in the borehole were accumulated on the surface. Generally, this limits the application of the method to the upper half of the borehole.
For the integration, we follow Raymond and others (1996), but along a trajectory along the velocity field, starting at point A at the surface and ending at point B somewhere in the borehole,

$$h_{\mathrm{A}}^{\mathrm{w.e.}} = k^{\mathrm{w.e.}}\, h_{\mathrm{B}} = \frac{\rho_{\mathrm{A}} w_{\mathrm{A}}}{\rho_{\mathrm{w}} w_{\mathrm{B}}} h_{\mathrm{B}} \qquad (2)$$

By multiplying measured annual layer thicknesses with the “water equivalent” thinning factor $k^{w.e.}$ in Eq. (2), the modeled annual layer thicknesses are obtained as a reconstruction of the accumulation rate history. It is interesting to note that under the given assumptions, the determination of the density profile in the borehole is not required. The Figure compares uncorrected and the corrected layer thicknesses in water equivalent.

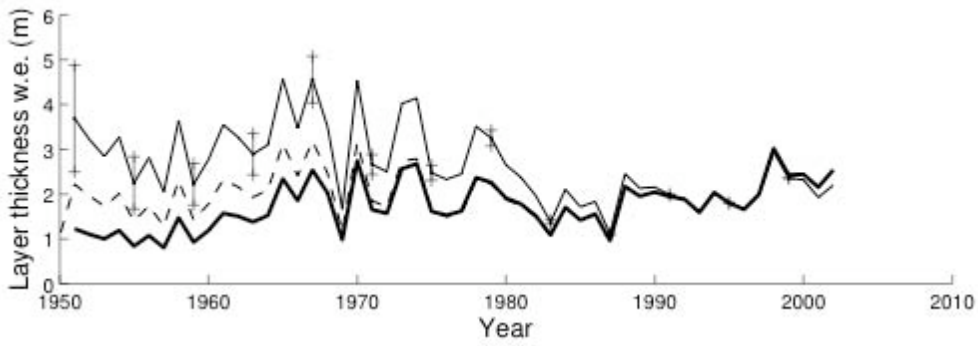

Figure. Thick solid line: measured annual layer thicknesses as a function of depth in water equivalent. Thin solid line: reconstruction of the accumulation rate history by multiplying the measured values with thinning factor $k^{w.e.}$ (with error bars). Dashed line: reconstruction of the accumulation rate history with the Nye (1963) correction.

References

C. F. Raymond and B. Weertmann and L. Thompson and E. Mosley-Thompson and D. Peel and R. Mulvaney, 1996: Geometry, motion and mass balance of Dyer Plateau, Antarctica, J. Glaciol., 42(142), 510-518

H. Bader, 1954: Sorge's law of densification of snow on high polar glaciers, J. Glaciol., 2, 319-323

A. S. Palmer and M. Schwikowski and T. Jenk and H. W. Gäggeler and A. Schwerzmann, 2004: Preliminary results from the 2002 Fiescherhorn ice core, Swiss Alps, Paul Scherrer Institut, Villingen, Switzerland, Annual report 2003. pp. 29

J. F. Nye, 1963: Correction factor for accumulation measured by the thickness of the annual layers in an ice sheet, J. Glaciol., 4(36), 785--788

J. F. Nye, 1975: Deducing thickness changes of an ice sheet from radio-echo and other measurements, J. Glaciol., 14(70), 49-56

ELEVATION CHANGE OF THE WEST GREENLAND ICE-SHEET MARGIN NEAR KANGERLUSSUAQ 2000-2003

ANDREAS P. AHLSTRØM[1], NIELS REEH[1], LARS STENSENG[2] AND RENE FORSBERG[2]

[1]Ørsted-DTU, Technical University of Denmark, Ørsteds Plads, Building 348, DK-2800 Kgs. Lyngby, Denmark
[2]Department of Geodynamics, Danish Space Center, Juliane Maries Vej 30, DK-2100 Copenhagen, Denmark

Abstract
Surface topography data acquired by laser scanning altimetry during the airborne campaign over the western Greenland ice-sheet margin in August 2003 was compared to a laser altimetry survey carried out over the same region in August 2000. For each point in the 2000 data set, a search was performed in the 2003 data set to find points within a horizontal search radius of 5 meters. The points found were then divided in four quadrants and used to make a weighted means interpolation to obtain an elevation estimate from 2003 at the point of the 2000 observation. The distributed data set resulting from this comparison provides a relatively complete picture of the ice sheet surface elevation change over a 50x50 km area of the ice margin and also serves as input to mass balance modeling. The elevation change data set arising from this comparison shows a mean thinning of roughly 0.5 meters from 2000 to 2003. The southernmost area shows a clear pattern of overall thinning, whereas the northernmost area shows a more variable pattern of moderate thinning and less pronounced thickening. An outline of the intended use of this data in a dynamic approach to mass-balance modeling will be presented as work in progress.

Introduction
Measuring the mass balance of the Greenland Ice-Sheet presents a formidable logistical challenge due to its vast size and the limited representability of individual stake measurements. It is therefore desirable to develop methods making it possible to estimate the mass balance from remote sensing. One way to do this is based on the application of the principle of mass conservation (Reeh and others, 2003). If the ice thickness h and horizontal surface velocity $u = (u_x, u_y)$ is measured once and the ice surface elevation S is measured and subsequently remeasured after some time Δt, then it is possible to derive the mass balance b_s of the intervening period by assuming a relationship $F=\underline{u}/u$ between the surface velocity and the mean velocity $\underline{u}$ of the underlying ice column, as expressed by the mass-conservation equation

$$\frac{\partial S}{\partial t} = b_s - \left(\frac{\partial (F h u_x)}{\partial x} + \frac{\partial (F h u_y)}{\partial y} \right)$$

This method has earlier been applied on the centre flowline of Storstrømmen Glacier in northeast Greenland (Reeh and others, 1999; Reeh and others, 2002), but has not yet been applied to the ice-sheet on a regional scale. The results presented here documents our progress towards obtaining this goal by presenting the current state of the necessary input data and showing new results obtained regarding the surface elevation change of the ice sheet.

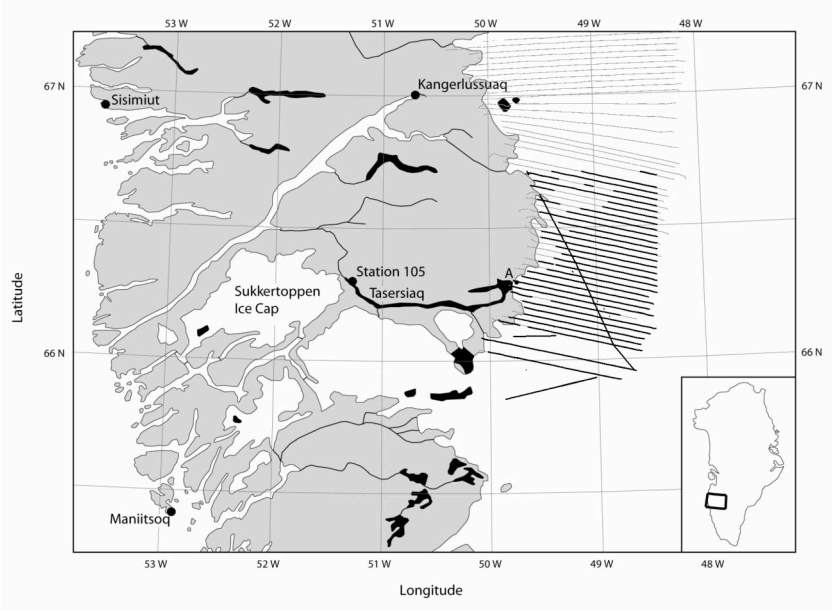

Figure 1. Overview of the region showing the flight tracks of the 2003 survey over the Greenland ice-sheet margin. The black flight lines show which part was used to produce the bed elevation model seen in Figure 5. The black lines also shows the area covered by the 2000 survey for which elevation change (see Figure 4) has been calculated. The figure is adapted from Ahlstrøm and others (in press).

Data collection and results

To facilitate a regional application of the mass-conservation principle, airborne campaigns have been launched in 2000 and 2003 (and will be repeated in 2005) to measure the ice-sheet surface elevation and thickness along a stretch of ice-margin 50 km wide and nearly 150 km long near Kangerlussuaq, West Greenland (see Figure 1). The ice-sheet surface elevation was determined by combining data from a laser altimeter (Optech ADM GPA100), two onboard differential GPS instruments and an inertial navigation system to keep track of the aircraft attitude. The laser altimeter used in 2000 was nadir-looking and acquired data at a 50 Hz rate which was subsequently averaged to 1 Hz yielding points with approx. 70 m along-track distance at the normal operation aircraft speed of 250 km/h. The laser altimeter used in 2003 was a scanning instrument, acquiring a dense swath of data with a width depending on the altitude of the aircraft above the surface, but

typically of a few hundred metres (see Figure 2 to compare the density of data points from the 2000 and 2003 surveys). The density of the scanner data is on the order of a metre between points, implying that a large amount of data is created.

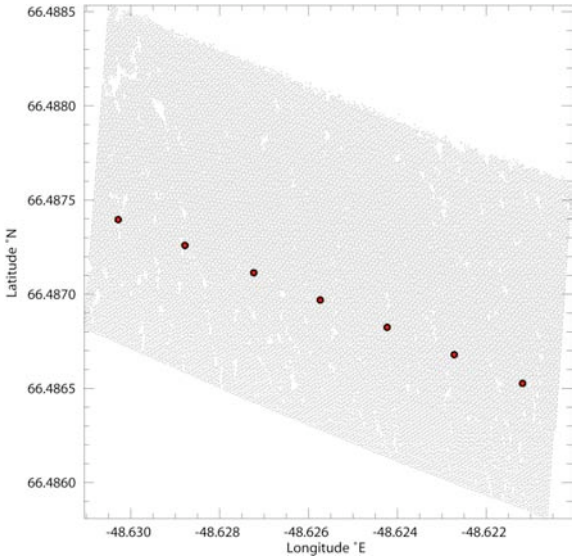

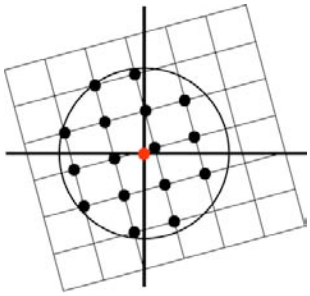

Figure 2 (left). Comparison of the averaged data density of the laser altimetry from the 2000 survey (fat red dots) and the 2003 survey (the light grey mesh). The real density from the 2000 survey is approximately one point per 1.4 m at normal flight speed, whereas the averaged data points from 2000 shown in the figure are roughly 70 m apart.

Figure 3 (right). The red dot signifies the averaged nadir data point from 2000, and the grid represents the scanner data from 2003. To interpolate a point from the 2003 data over the location of the 2000 data point, all scanner-data points within a search radius of 5 m were selected, averaged within four quadrants which were finally linearly interpolated.

The data was checked by comparing data from several crossing flight lines and those with obvious errors identified were discarded. Repeated laser altimetry currently provides the most accurate feasible method to map ice-sheet surface elevation change over a larger area. In this case we compared the two laser altimetry data sets, by choosing available scanner data points from 2003 in a radius of 5 m around each averaged nadir data point from 2000. The selected 2003 data were then grouped into four quadrants and finally linearly interpolated to the location of the single 2000 data point (see Figure 3). Elevation changes over 5 metres obtained with this method were ignored to discard areas with crevasses and highly irregular topography. For the area covered by both the 2000 and the 2003 survey, a total of 7303 usable points were identified. With the survey in 2005 we will be able to compare to laser scanner data sets, producing a very dense data set of elevation change which might be of interest in studying details in the

changes of the ice-sheet surface topography. The calculated along-track elevation change was gridded to a resolution of 250 m using the method 'inverse distance to a power two' with subsequent smoothing, producing the map shown in Figure 4, which also shows the actual points used. The accuracy of the two data sets has not yet been adequately analyzed, but is expected to be within 0.25 m for the 2003 data set (Kristian Keller, personal communication). The accuracy of the nadir laser altimetry data from 2000 has previously been assessed in a cross-track analysis by Howe Ditlevsen (2001).

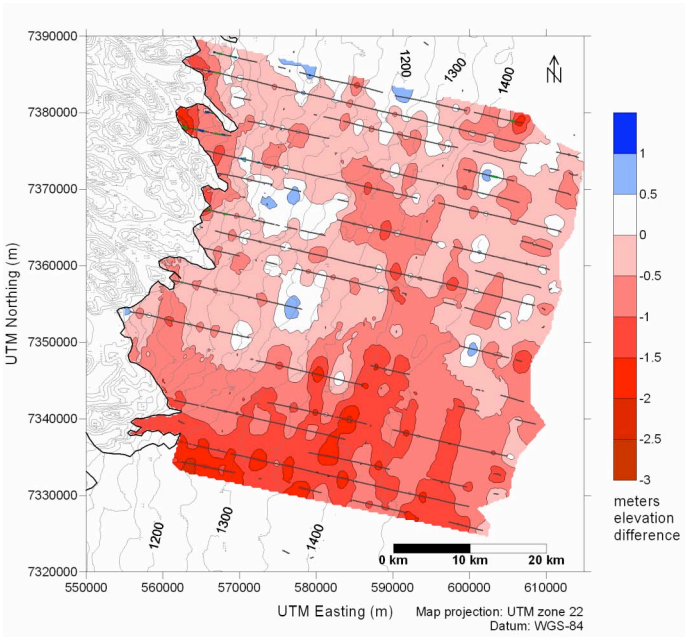

Figure 4. Contoured map of the observed elevation change of the ice-sheet margin from 2000 to 2003. The thick grey points (seen as lines) show the location of the data points used in the grid interpolation. The light grey contours show the elevation above sea level. See the text for a discussion of the resulting pattern of elevation change.

Even though the laser altimetry provides the basis for a digital elevation model (DEM) of the ice-sheet surface, the satellite-derived alternative provided by repeat-track interferometric synthetic aperture radar (InSAR) analysis is preferable for use in a mass-conservation calculation because of its distributed high resolution. The laser altimetry can then be used to independently check the accuracy of of the InSAR DEM. Such a DEM was derived from two image pairs from the satellites ERS-1 and ERS-2 acquired from October 1995 to January 1996 during the twin mission and is shown in Figure 5. A comparison with a DEM based on the nadir laser altimeter data from 2000 gave a mean difference of 5 metres with an r.m.s. of the difference of 10 metres (Ahlstrøm and others, 2002). The DEM shown in Figure 5 has a reduced resolution of 250 metres to conform to the bed elevation model described below. The repeat-track InSAR analysis also yields a line-of-sight

surface velocity component which can be combined with glaciologically based assumptions to provide an estimate of the surface velocity field (u_x, u_y) needed in the mass-conservation equation (Mohr and others, 2003). An example of the derived surface velocity field from an outlet glacier in the region studied is shown in Figure 6.

Ice-sheet thickness was obtained by manual interpretation of radargrams collected during the airborne survey in 2003 with the 60 MHz ice-penetrating radar of the Technical University of Denmark (Christensen and others, 2000). The ice-sheet thickness data was reduced to an along-track resolution of 200 metres and converted to a gridded digital elevation model using block kriging with eight directional semi-variograms to take into account the influence of the dominant valley systems beneath the ice sheet on the gridding result (Ahlstrøm and others, in press). The grid resolution was chosen to be 250 metres as a compromise between the high along-track resolution, typically on the order of a metre and the between-track distance of roughly 2500 metres. The resulting grid is displayed as a contour map in Figure 5.

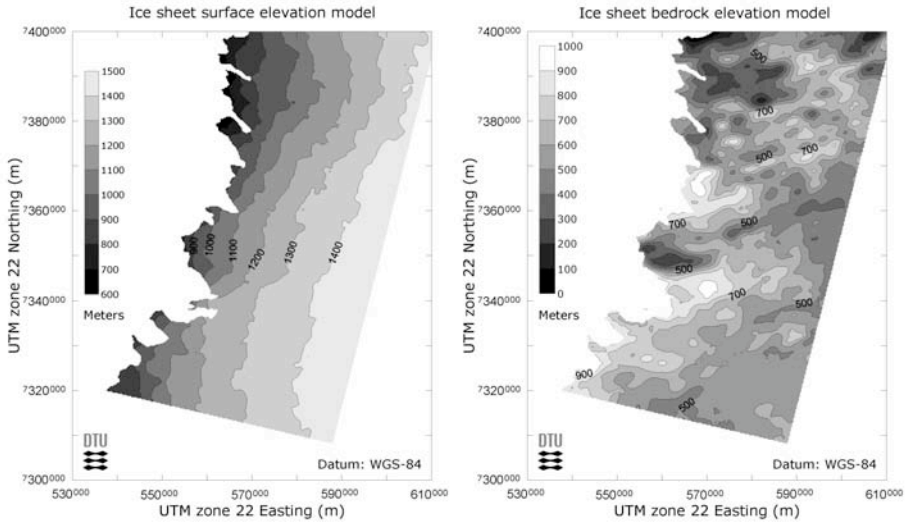

Figure 5. The left side shows a digital elevation model based on satellite-derived repeat-track interferometric synthetic aperture radar analysis. The right side shows a digital elevation model of the bed underneath the ice sheet, based on an airborne ice-penetrating radar survey in 2003. The figure is adapted from Ahlstrøm and others (in press). The contours are in metres above sea level.

Conclusion and Outlook

The results are presented here as work in progress towards the application of the mass-conservation principle to model the mass balance of the Greenland ice-sheet margin on a regional scale. However, an interim product such as the observed elevation change deserves attention in its own respect. The map shown in Figure 4 gives a detailed picture of the observed elevation change of a 50x50 km part of the

Greenland ice-sheet margin over three years in a region which has been reported to be sensitive to climate change (Huybrechts and others, 1991). Even though work still has to be done to assess the accuracy of the laser altimetry data, it still represents the best estimate currently available.

The mean observed elevation change from August 2000 to August 2003 over the whole region shown in Figure 4 is -0.5 metres. However, the change is not uniformly distributed: the northern and central parts seem to be in balance, whereas the southern part is thinning. The thinning of the ice sheet in the southern part of the region studied is a robust result even when considering the uncertainty in the accuracy of the laser altimetry data. The survey was carried out by the end of the ablation season in late August in both 2000 and 2003, minimizing the influence of snow on the result. The region is situated in a precipitation shadow from coastal ice caps and mountains and receives relatively little snow. The snow line is likely to be as high as 1400 m a.s.l. at the time of the survey assuming that it is comparable to the equilibrium line elevation. The elevation change pattern seen in Figure 4 does not show any elevation dependency and remains to be explained. Possible candidates are increased surface ablation, a change in the precipitation or ice-dynamical changes. The latter could be influenced by a portion of the margin draining into an ice-dammed lake (provisionally named 'Lake 860' from its elevation signature on maps) known to drain catastrophically with intervals of several years.

Further work includes InSAR processing of large image strips from both ascending and descending satellite tracks, providing two surface velocity vectors instead of just one as is currently available. The InSAR-derived surface velocity which represents a winter snapshot should be compared to stake velocities obtained within the region, along the K-transect near Kangerlussuaq and near the lake Tasersiaq. A more detailed error analysis of the laser altimetry data is also required, both for the nadir data from 2000 and the scanner data from 2003. Finally, mass-balance modeling using the outlined mass-conservation method will be applied and compared to results from distributed surface ablation modeling and ablation measurements from stakes.

Acknowledgements

This research was funded by the EU under EC-5FP contract EVK2-2001-00262 (Space borne measurements of Arctic Glaciers and implications for Sea Level - SPICE). The European Space Agency owns the copyright to the ERS-1 and ERS-2 images.

References

Ahlstrøm, A. P., C. E. Bøggild, J. J. Mohr, N. Reeh, E. L. Christensen, O. B. Olesen, K. Keller. 2002. Mapping of a hydrological ice-sheet drainage basin on the West Greenland ice-sheet margin from ERS-1/-2 SAR interferometry, ice-radar measurement and modelling, Ann. Glaciol., Vol. 34, 309-314.

Ahlstrøm, A. P., J. J. Mohr, N. Reeh, E. L. Christensen and R. LeB. Hooke. In press. Controls on the basal water pressure in subglacial channels near the margin of the Greenland ice sheet, J. Glaciol. (accepted).

Christensen, E. L., N. Reeh, R. Forsberg, J. H. Jørgensen, N. Skou, K. Woelders. 2000. A low-cost glacier-mapping system, J. Glaciol., 46(154), 531-537.

Howe Ditlevsen, E. 2001. Højdebestemmelse af isranden syd for Kangerlussuaq med kinematisk GPS og flybåren laseraltimetri samt sammenligning, Speciale (MSc thesis), University of Copenhagen.

Huybrechts, P., A. Letréguilly, N. Reeh. 1991. The Greenland Ice Sheet and greenhouse warming, Palaeogeog. Palaeoclimatol. Palaeoecol., Vol. 89, 399-412.

Mohr, J. J., N. Reeh, S. N. Madsen. 2003. Accuracy of three-dimensional glacier surface velocities derived from radar interferometry and ice-sounding radar measurements, J. Glaciol., 49(165), 210-222.

Reeh, N., S. N. Madsen, J. J. Mohr. 1999. Combining SAR interferometry and the equation of continuity to estimate the three-dimensional glacier surface-velocity vector, J. Glaciol., 45(151), 533-538.

Reeh, N., J. J. Mohr, W. B. Krabill, R. Thomas, H. Oerter, N. Gundestrup and C. E. Bøggild. 2002. Glacier specific ablation rate derived by remote sensing measurements, Geophys. Res. Lett., 29(16), 10-1 – 10-4.

Reeh, N., J. J. Mohr, S. N. Madsen, H. Oerter and N. Gundestrup. 2003. Three-dimensional glacier surface velocites of Storstrømmen glacier derived from radar interferometry and ice-sounding radar measurements, J. Glaciol., 49(165), 201-209.

COMPARATIVE SIMULATIONS OF SNOW AND SUPERIMPOSED ICE AT THE KONGSVEGEN GLACIER, SVALBARD

STEFAN ERATH[1], FRIEDRICH OBLEITNER[1], JACK KOHLER[2], WOUTER GREUELL[3] AND KJETIL MELVOLD[4]

[1] Institute for Meteorology and Geophysics, Innsbruck University, Austria
[2] Norwegian Polar Institute, Tromsoe, Norway
[3] Institute for Marine and Atmospheric Research Utrecht, Utrecht University
[4] The Norwegian Water Resources and Energy Directorate, Oslo

Abstract

We consider glaciological and meteorological data that were collected at about the equilibrium line of a high Arctic glacier (Kongsvegen, Svalbard). The study is based on detailed investigations of the seasonal evolution of the local mass and energy budget of the glacier, where snow modeling turned out to be a valuable tool. Amongst the particular aspects the formation of multi-year superimposed ice has been focused, which has important implications on the mass balance of this glacier.

This study is of a more methodical nature addressing the potential of three different snow models (SNOWPACK, SNTHERM and SOMARS) to reproduce the local development of snow and ice at this site. Their skill is mainly measured in terms of profile characteristics of snow temperature and density and their temporal evolution. These verifying data confirm that principally each model is well able to simulate the basic features observed. Focusing on the performance of SOMARS we demonstrate the importance of properly derived precipitation input and corresponding impact on the simulation results. A corresponding procedure to ensure a basic model comparability is introduced. The largest differences between the model results and measurements occur in the near surface layers (±1.5°C and ±70 kg m^{-3}), which is acceptable in view of the limited tuning effort and the inherent measurement uncertainties. Amongst the common notable lacks in skill, the standard versions of these models systematically underestimate the development of superimposed ice. Moreover, none of these models does reproduce a detailed structure of the snow layering. We note however, that depending on fine-tuning effort each model has a similarly high potential to overcome the demonstrated lacks in skill.

Introduction

Kongsvegen is a high arctic polythermal glacier with an area of 102 km^2 and 25 km length. A surface cold layer reaches the bedrock in the ablation area where the glacier is partly frozen to the ground. The ice is mostly temperate in the higher basins where the formation of superimposed ice is an important factor regarding the energy and mass budget of the glacier (Lefauconnier et al., 1999). Glaciological and meteorological data have been collected at about the equilibrium line of Kongsvegen glacier (79°N, 13°E, 543 m asl). The basic meteorological parameters are measured as well as the short- and longwave radiation

components, snow height and snow temperatures at different depths. During the twice-yearly maintenance of the station, detailed glaciological investigations of the snow and ice conditions were performed as well. Covering several annual cycles meanwhile (2000-2004), these data allowed for process oriented investigations of the multi-year evolution of the local mass and energy budget of the glacier (Obleitner and Lehning, 2004). The current study is of a more methodical nature and focuses on the comparative skill of different snow models to simulate the development of snow and ice at the site of investigation. A special emphasis is put on the performance of SOMARS (Greuell, 1994).

The environmental regime

Radiation exerts the dominant forcing on the energy budget at this site, with polar night conditions from late October through early February. The air temperatures can be as low as -40°C, but the winter regime is coreless due to the vital synoptic activity enforcing episodic break ups of the otherwise persistent radiation inversions. The summer temperatures settle around 0°C, which can be attributed to the stabilizing influence of melting snow and ice. The wind regime is characterized by moderately developed glacier winds, which are influenced by topography and synoptic disturbances. Moreover, the site is characterized by a cold, 1.5 to 2 m deep snow pack at the end of winter. Intensive melt usually starts in May, when the formation of superimposed ice is initiated too. At this elevation and with the current climate conditions, there is multi-year formation of superimposed ice, but the final amount strongly depends on the individual summer conditions and the micro-topographical conditions at the snow-ice interface (Obleitner and Lehning, 2004). During certain summers, superimposed ice was observed to build up in abnormally large extent (up to 0.5 m), which has important implications on the mass balance of the whole glacier.

Model setups

We investigate the skill of three well known snow models SNOWPACK, SNTHERM and SOMARS (Bartelt and Lehning, 2002; Jordan, 1991; Greuell, 1994) to reproduce the seasonal evolution of the physical properties of snow and ice at the measurement site. The respective skill of a specific version of SNOWPACK (6.1) has already been documented (Obleitner and Lehning, 2004). Here, special emphasis is given to SOMARS, which is intended to be used for distributed mass balance modeling of Spitzbergen glaciers. It is advantageous in the context of a comparative study that each model can be fed with the same basic input. Their numerical setup considers 25m of ice upon which the evolution of seasonal snow is initialized with measured profiles of snow temperature and density. Thus starting in April 2000 the governing boundary layer processes are driven by the measured meteorological data. We use hourly values of air temperature and humidity, wind speed, short-wave incoming and reflected radiation and long-wave atmospheric radiation. In a first approach, precipitation input was derived from filtered ultrasonic records, which was converted into water equivalent using a constant new snow density of 150 kg m^{-3}. Due to differences in the treatment of metamorphosis and settling processes, however, model specific adjustments turned out to be necessary order to yield the correct snow height at the end of winter. Shortly recalling the relevant model characteristics, SNOWPACK's metamorphosis routine is based on microstructure parameters and accumulation is added if measured

snow height is less than the simulated one. Naturally, such forces the model to reproduce the correct amount of snow height. SNTHERM uses a densification parameterization, which is based on grain size and temperature. The original version of SOMARS on the other hand uses a less sophisticated settling routine, which might be sufficient for certain applications. In the context of our local studies, however, we experienced serious deficiencies to reproduce the observed evolution of snow and SOMARS was modified by partly adopting SNTHERM's parameterization. To summarize, the accumulation input procedures are slightly different for each model, however, force them to reproduce the measured snow heights within ±15 cm. This is essential for proper modeling of snow processes and for model comparison, too. Profiles of density (water equivalent) and temperature from annual snow pit data and records of snow temperature at certain depths were taken as measures of verification.

Results of SOMARS simulations

We firstly document the importance of properly derived accumulation input on the simulation results, which is a general issue for snow modeling. In this context filtering of the original ultrasonic records is a crucial issue, which in our case was done by the application of reasonable thresholds ruling out obvious disturbances of the signal. Moreover, the assumption of a new snow density (150 kg m^{-3}) is necessary in order to deduce water equivalents as input into the model. There is no general rule for this as there is a high natural variability (e.g. snow drift effects) and as e.g. the model specific parameterization of the initial settling processes plays a role there, too. In a first attempt an "effective" new snow density (350 kg m^{-3}) was introduced to SOMARS. Figure 1 demonstrates, that such works reasonably

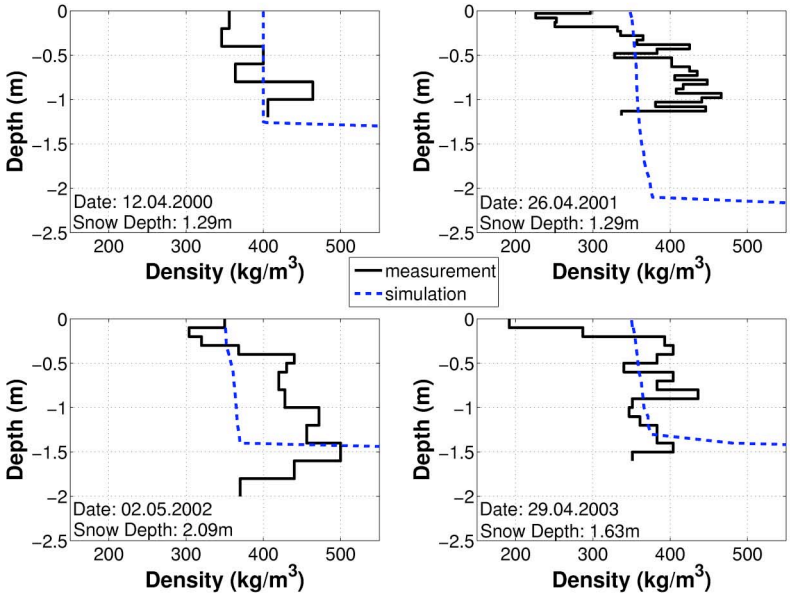

Figure 1. Measured and modeled snow density at the end of the accumulation period in successive years 2000 – 2004, straightforwardly feeding SOMARS with filtered measured ultrasonic data.

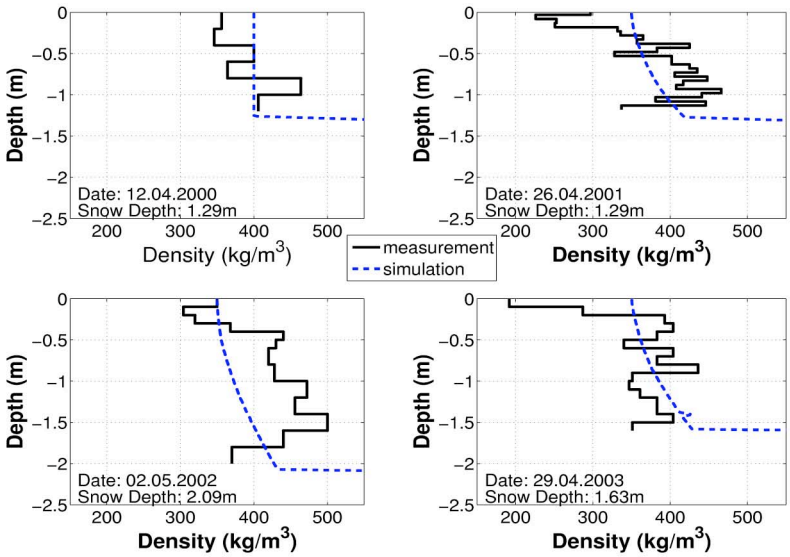

Figure 2. Measured and modeled snow density from 2000 – 2004, feeding SOMARS with filtered ultrasonic data, which are scaled by end winter accumulation observed in snow pits.

during certain accumulation periods (winter 2003), whereas unacceptable lacks in skill are left with respect to winters 2001 and 2002, respectively. Of course there is an inherent natural variability to be considered as well, but the main deficiencies appeared due to improper derivation of accumulation input. It is obvious at this point already, that additional glaciological data (like snow pits) are essential in order to rule out the inherent problems.

We have tested different methods to improve these first results. Different filtering methods and new snow density algorithms yielded partly reasonable results, which mostly suffered from a wide lack in objective criteria on the other hand. In this view we finally preferred to simply scale the pre-filtered ultrasonic records by the end winter accumulation observed in snow pits. Figure 2 documents the corresponding improvement in reproducing the observed annual accumulation.

Snow height, as well as overall density is well simulated now, however, there is still an obvious lack in reproducing the layered structure. Gustafsson et al. (2004) have demonstrated that such is a common deficiency of other snow models as well. In the case of SOMARS, this is definitely due to a rather insufficient treatment of snow metamorphosis processes. It is to be noted in this context moreover, that for the purpose of this study a new densification algorithm according to Jordan (1991) has been implemented into SOMARS.

A thus optimized accumulation input yields otherwise reasonable results a well. Figure 3 shows comparisons of simulated snow temperature profiles with measurements in annual snow pits. There is a basic agreement matching the experiences with other models (Obleitner and Lehning, 2004). The larger deviations in the uppermost layers may also be attributed to measurement

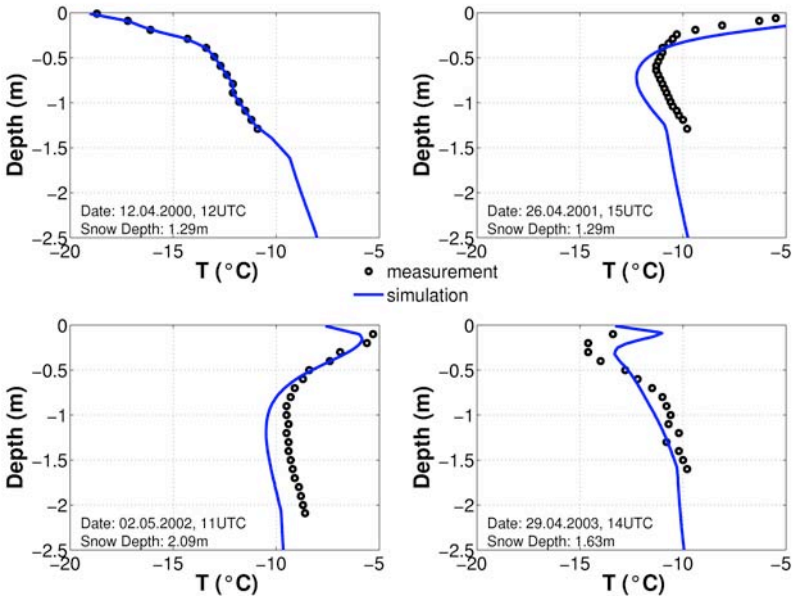

Figure 3. Measured and modeled snow temperature from 2000 – 2004, feeding SOMARS with ultrasonic data scaled by end winter accumulation observed in snow pits

problems (solar heating of sensors) or insufficient temporal coincidence (mean hourly values vs. instant values).

A thus verified model run shows some generally interesting features of the seasonal evolution of snow and ice at the site of investigation. Snow height in the end of winter varied between 1.3 and 2.1 m during the 4 years of investigation corresponding to 53 to 75 cm w.e., respectively. Ablation usually takes place during the period mid June until mid September. The calculated annual specific mass balances (1 Oct. – 30 Sep.) range from +0.08 m w.e (2002) to -0.32 m w.e (2003). The annually different winter and summer conditions are largely reflected in the temperature and precipitation of a nearby climate station in Ny Alesund (78°53'N, 11°80'E) and there are obvious consequences on the penetration of the winter and summer heat waves into the ice below. Figure 4 indicates that throughout the years the winter coldness systematically penetrates deeper into the underlying ice layers. Partly, this can be related to subtle interaction between atmospheric development and the depth of snow at the relevant period of time. As an example, the most intensive cooling occurs relatively early during autumn 2004, when little snow covers the glacier on the other hand. Another factor in this context is that during the period of concern the ice surface continuously lowers due to prevailing net ablation. Therefore, an ice layer at a certain reference depth is increasingly exposed to the approaching cold wave.

By contrast, the depth of summer heat wave penetration remains relatively constant. This can be related to phase changing processes modifying the conductive effects. The governing factors are production and refreeze of melt water, which basically depend on length and climatic conditions of the melt period,

as well as on the cold content of the underlying ice on the other hand. The polar day conditions imply effective production of melt water. The latter penetrates the snow pack within short periods of time and refreezes at the cold snow ice interface of the glacier.

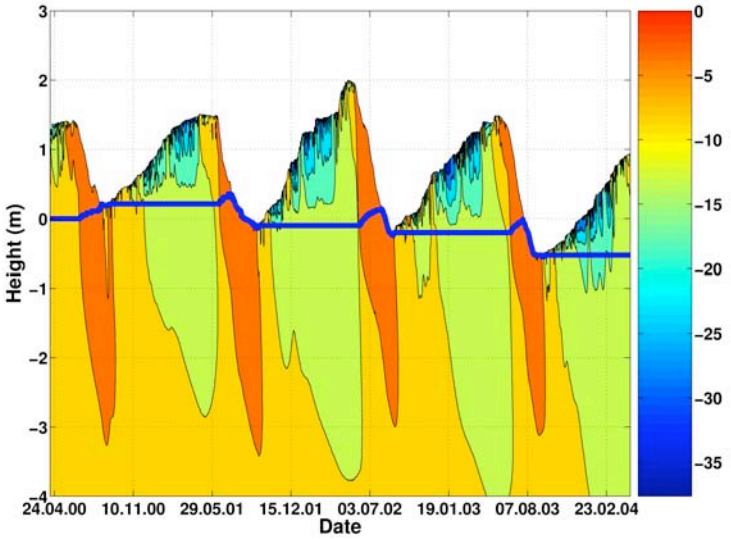

Figure 4. Contour plot of simulated snow and ice temperatures (°C) during April 2000 –April 2004. The thick (blue) line indicates the snow ice interface.

It has been demonstrated that considerable amounts of superimposed ice are thus developing at the Kongsvegen measurement site (Obleitner and Lehning, 2004). This study has shown moreover, that the local slope and the micro-topographical conditions at the snow/ice interface of the glacier may play an additional role in determining the final amount of superimposed ice. In extreme cases, the melt water can intermittently form ponds, resulting in abnormally high stocks of superimposed ice. Depending on these factors there is an inherent local and temporal variability of such effects, which are important for the thermal regime and the mass balance of the glacier.

Figure 4 proves that SOMARS is reasonably reproducing the changes in surface height at the measurement location. Net ablation as well as the annually developing amount of superimposed is confirmed by different measurements at the site. A major deviation regards the amount of superimposed ice formed during summer 2000, when abnormally high amounts of superimposed developed due to ponding water phenomena (Obleitner and Lehning, 2004). SOMARS includes a parameterization of slope and time dependent runoff at the snow/ice interface, which in principle could be used to reduce runoff at the ice/snow interface. However, we did not correspondingly optimize the SOMARS run within this study.

Snow model intercomparisons

The available data provide a most suitable basis for a verified comparison of the results from different snow models. We used SOMARS, SNTHERM and SNOWPACK, which are well documented and state of the art representatives. For the purpose of this study we used the currently available versions of each model and there was no model specific fine-tuning. Note however, that SOMARS has been modified by the mentioned densification routine. The models were fed by the same meteorological and glaciological input data and their basic skill is measured focusing on snow density and temperature profiles. The conditions at the snow/ice interface are essentially interesting, as being considered to critically react on proper treatment of the relevant processes transferring mass and energy between the atmosphere, snow (above) and ice (below).

There are a number of factors that are hampering a straightforward comparison of the model results. This was an experience of the SNOWMIP intercomparison effort as well (Essery, 1998). Thus, we have already noted the importance of model specific treatment of precipitation input (effective new snow density?), which has important impacts on proper reproduction of snow height affecting the temperature and density distribution as well. Moreover, the models use different methods to distinguish the precipitation phases (snow or rain?). As to the verifying data, we note the inherent measurement uncertainties, which may be estimated to ±50 kg m^{-3} and ±0.5 °C at least. Further uncertainty exists regarding geometrical references between measurements and model results (e.g. 5 cm volume increments of density measurements vs. nodal values of changing thickness, depth of pit vs. depth of model snow pack). Some of these problems can certainly be overcome by fine tuning individual model runs or developing specific post-processing tools allowing for better comparison of measurements and simulation results. As a minimum requirement however, we took care that each model reproduces the end winter snow height to within ±15 cm. The SOMARS runs were most optimized with that respect while corresponding effort regarding SNTHERM and SNOWPACK was beyond the scope of this study.

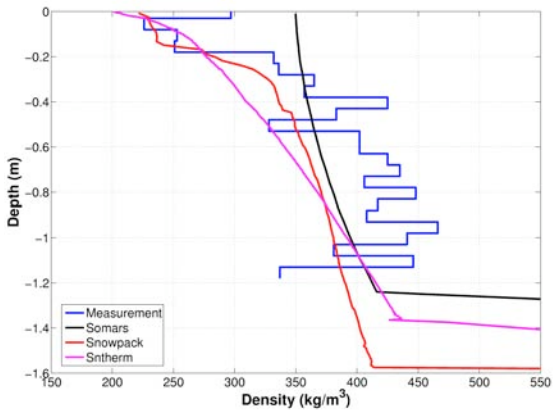

Figure 5. Comparison of density profiles as measured in a snow pit and simulated by SOMARS, SNTHERM and SNOWPACK, respectively (26 April 2001, 15UTC).

Figure 5 compares the measured and simulated snow density profiles. Considering the inherent measurement uncertainty, the overall level as well as densification with depth is reasonably captured by each model. In the uppermost layers, however, SNTHERM and SNOWPACK perform better than SOMARS, which is due to their more sophisticated treatment of snow metamorphism processes and the lower values of effective new snow density. In the central layers the models tend to underestimate the measured snow density. As a common feature as well, none of the considered models reproduces a detailed layered structure of the snow pack. This indicates a general lack of these models and a corresponding need for improvement (Gustafsson et al., 2004; Obleitner and Lehning, 2004).
Figure 6 compares the simulated snow temperature profiles with the measurements in the snow pit. The inherent measurement uncertainty is difficult to estimate e.g. due to solar heating of the sensor in the uppermost layers for instance. A value of ±0.5°C might be considered as a minimum estimate in this context. In view of this, the models do reasonably reproduce the overall shape of the measured temperature profiles. However, the simulated average temperature of the snow pack differs within a range of 3°C. SNTHERM and SOMARS tend to be too cold and SNOWPACK is calculating too warm on the other hand. Moreover, SOMARS simulates the temperature minimum at greater depth as observed. This might be related to the relatively large new snow density (350 kg m^{-3} as compared to 150 kg m^{-3}) and correspondingly enhanced penetration of the winter cold wave into the deeper snow layers.

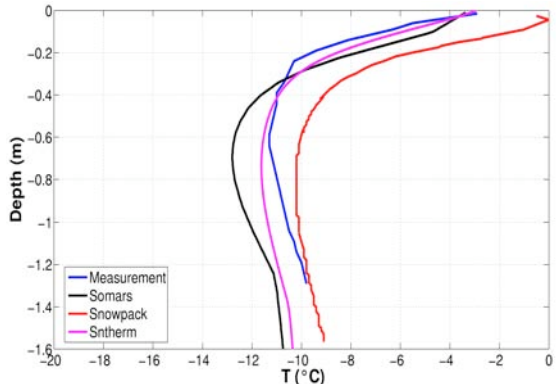

Figure 6. Comparison of snow temperature profiles as measured in a snow pit and simulated by SOMARS, SNTHERM and SNOWPACK, respectively (26 April 2001, 15UTC).

It has been mentioned that the thermal conditions at the snow/ice interface are particularly interesting, as critically responding on proper treatment of the relevant processes transferring mass and energy between the atmosphere, snow and ice. The formation of superimposed ice plays an important role in this context too, which has a great potential to effectively modify the thermal regime in these layers. Figure 7 documents the model's ability to simulate the time evolution of the temperature at the snow-ice interface. Generally, the model results agree to within about ±1°C to the verifying data and the major deviations can mostly be related to

documented measurement problems. The arrival of spring melt water (0°C) at the snow-ice interface may be considered as another interesting measure of skill. In spring 2000 for example, this was recorded on 27 June. SNTHERM and SOMARS do well reproduce this date (26 June). This is surprising in view of the manifold dependences including history of the development of winter snow and different parameterization of water transport within the snow pack. SNOWPACK's water arrives 7 days later, which is mainly due to having simulated a too cold winter snow pack. On the other hand the performance of this simulation has already been improved by modifying the water transport routine to treat ponding of melt water. Abnormally large amount of superimposed ice were thus formed during the subsequent summer 2000, which could successfully be simulated (Obleitner and Lehning, 2004). SOMARS and SNTHERM have not been optimized with that respect, thus tend to underestimate the amount of superimposed ice during this particular summer (2000). This may be considered as a reason for simulating comparatively low temperatures during the following spring 2001 (Figure 6).

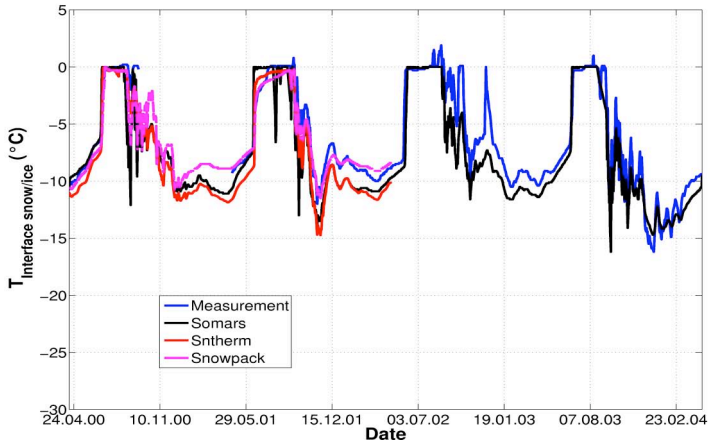

Figure 7. Comparison of measured and simulated temperature at the snow-ice interface. The SNOWPACK and SNTHERM simulations cover a shorter period only (April 2000 until April 2002).

Summary

Three state of the art snow models (SNOWPACK, SNTHERM and SOMARS) have been fed with the same set of meteorological and glaciological input data. The measurements cover a four year period and have been collected at about the current equilibrium line of Kongsvegen, which is a high Arctic polythermal glacier in western Spitzbergen. The formation of superimposed ice is a particularly interesting aspect there.

Focusing on the performance of SOMARS mainly, the basic importance of proper derivation of precipitation input is demonstrated firstly. This is based on ultrasonic records, which were pre-processed to match the snow depth of pits dug at the end of each winter. Conversion into water equivalents was achieved by the application of an "effective" new snow density. Different values (ranging from 150 to 350 kg m^{-}

^{3}) were necessary in order to force each model to reproduce the observed winter mass balance, which is related to the model specific parameterizations of initial snow compaction processes. This procedure is effective and facilitates comparison of the model outputs. SOMARS was further optimized by adopting parts of the settling routine of SNTHERM and scaling precipitation input to the observations in snow pits at the end of winters. The original versions of the models were used otherwise, with exception of SNOWPACK, whose water transport routine was modified to treat ponding water effects. There was no specific fine tuning of the simulation result towards the verifying observations.

The model's skill is mainly measured by comparison with data from annually available snow pit data and continuous records of snow temperatures at the snow-ice interface. The verifying data from a test pit at the end of winter 2000 demonstrate that each model is well able to reproduce the overall evolution of the snow pack. The inter-model differences in simulated snow temperature are in the range of ±1.5°C, which are mostly systematic throughout the depth of the snow pack and must be seen in the light of an estimated measurement uncertainty in the order of ±0.5°C. We note that the models winter cold wave systematically penetrate too deep into the snow pack. This may indicate improper treatment of effective heat conduction, especially in the near surface layers.

The accuracy of the verifying density measurements is probably not better than ±50 kg m^{-3}. In view of this, the considered snow models capture the overall level and distribution with depth equally good. However, there are systematic deviations regarding the slope of the simulated density profiles. As compared to SOMARS, SNTHERM and SNOWPACK show stronger densification with depth (and time). This must be related to different parameterization of snow metamorphism, where the treatment of the processes immediately after snow fall may be of major importance. The largest inter-model differences occur in the near surface layers, where SNTHERM and SNOWPACK perform better than SOMARS reflecting a more sophisticated parameterization of the relevant processes. Reasonably, some of these features trace on the simulated temperature profiles as well. For instance, SOMARS simulates the densest and therefore the coldest snow pack. Such evidences call for further investigation of the inherent feedback processes, which was beyond the scope of this study. We finally note in this context, that none of the three models reproduces any detailed layered structure within the snow pack. This is another topic to be focused in further studies.

The multi-year evolution of the temperature at the snow–ice interface is considered as an important measure of the model's skill as critically responding to properly treating the relevant processes transferring mass an energy between air, snow and underlying ice. A comparison of model results with direct measurements demonstrates some systematic differences between the model results, which widely conform to the evidences from the profile investigations. Thus, SNTHERM and SOMARS are systematically to cold, whereas SNOWPACK performs optimally. The onset of spring melt is correspondingly affected. It is to mentioned in this context, however, that SNOWPACK has been optimized regarding the production of superimposed ice. The latter is a prominent feature at the measurement site with important consequences on the mass and energy budget of the glacier. The standard versions of the three models tend to produce too small amounts of superimposed ice (0.15 cm typically). On the other hand, SNOWPACK's water transport routine has been modified to reproduce the

generally larger amounts of superimposed ice, particularly during certain years (0.5 m during summer 2000, for instance). The accordingly enhanced release of latent heat might be a reason for SNOWPACK's higher temperatures in the layers of concern.

Amongst the factors hampering a straightforward comparison of the model results we note the model dependent treatment of precipitation input (effective new snow density?) or different methods to subsequently distinguish the precipitation phases (snow or rain?). As to the verifying data, we note the inherent measurement uncertainties and further uncertainties regarding geometrical references between measurements and model results (volume increments vs. nodal values of changing thickness, depth of pits vs. depth of model snow pack). Some of these problems can certainly be overcome by fine tuning individual model runs or developing specific post-processing tools allowing for better comparison of measurements and simulation results. Such was beyond the scope of this study and therefore corresponding outcome may not be misinterpreted in terms of attempting to provide absolute measures of the skill of individual models. No doubt, each of the considered models has a similarly high potential to be optimized, corresponding effort and support from the model developers provided. Nevertheless, some of the demonstrated features might be valuable for less experienced users or stimulate further investigations fostering progress in snow modeling.

Acknowledgements and remarks

Particular thanks are due to J. Oerlemans for organizing another "Pontresina-workshop" and for patiently waiting for input to these proceedings. The financial support by M. Kuhn is gratefully acknowledged as well.

The SOMARS calculations were performed by S. Erath as part of his diploma work and F. Obleitner contributed the SNTHERM and SNOWPACK simulations. The latter results were taken from a former study developed in cooperation with M. Lehning who provided the model and assistance in modifying its water transport module. Field work was performed in close cooperation with J. Kohler and K. Melvold, W. Greuell provided his model and valuable comments on its proper use..

References

Bartelt P. and M. Lehning: A physical SNOWPACK model for the Swiss avalanche warning, Part I: numerical model, Cold Regions Science and Technology, 35, 3, 123-145, 2002.

Essery R., E. Martin, H. Douville, A. Fernadez, E. Brun: A comparison of four snow models using observations from an alpine site , Climate Dynamics 15 :583-593,1998.

Greuell W. and T. Konzelmann: Numerical model of the energy balance and the englacial temperature of the Greenland Ice Sheet. Calculations for the ETH-Camp location (West Greenland, 1155m a.s.l.), Global and Planetary Change, 9, 91-114, 1994.

Gustafsson D., P. Waldner and M.Stähli: Factors governing the formation and persistence of layers in a subalpine snowpack, Hydrol. Process. 18, 1165–1183, 2004.

Jordan R.: A one-dimensional temperature model for a snowcover, CRRELL Spec. Rep., 91-16, 49p, 1991.

Lefauconnier B., Hagen J. O., Orbak J. O., Melvold K. and Isaksson E., Glacier balance trends in the Kongsfjorden area, western Spitzbergen, Svalbard, in relation to the climate, Polar Res., 18 (2), 307-313, 1999.

Obleitner F. and M. Lehning: Measurement and simulation of superimposed ice at the Kongsvegen glacier, Svalbard (Spitzbergen), J. Geoph. Res., 109, D04106, doi:10.1029/2003JD003945, 12pp, 2004.